THE UNIVERSITY OF MICHIGAN

COLLEGE OF ENGINEERING

Department of Aerospace Engineering

High Altitude Engineering Laboratory

Scientific Report

THE ADMITTANCE OF THE INFINITE CYLINDRICAL ANTENNA IN A LOSSY, ISOTROPIC, COMPRESSIBLE PLASMA

Edmund K. Miller

ORA Project 05627

under contract with:

NATIONAL AERONAUTICS AND SPACE ADMINISTRATION

CONTRACT NO. NASr - 54(05)

WASHINGTON, D. C.

administered through:

OFFICE OF RESEARCH ADMINISTRATION ANN ARBOR

March 1967

Acknowledgment

The author is grateful for the many stimulating and helpful discussions he had with Mr. Hal F. Schulte during the course of this work.

TABLE OF CONTENTS

LIST OF FIGURES

Abstract

Numerical values are presented for the admittance of an infinite cylindrical antenna excited at a circumferential gap of finite thickness and immersed in a lossy, isotropic, compressible plasma. The formulation uses the linearized hydrodynamic equations for the electrons (ion motion is neglected) together with Maxwell's equations. A free-space layer of finite, variable thickness (the vacuum sheath) is used to approximate the positive ion sheath which forms about a body at floating potential in a warm plasma. The antenna admittance is obtained by direct numerical integration of the Fourier integral for the antenna current, and is presented for plasma parameter values typical of the E-region of the ionosphere.

The results obtained show for the parameter range investigated that above the plasma frequency, the electron temperature, electron collisions and the sheath have relatively little influence on the admittance. Below the plasma frequency, the admittance is very dependent upon these parameters. In particular, a rather marked maximum in both the conductance and susceptance is found at about half the plasma frequency, which is not present when the sheath thickness and electron temperature are both zero. Of particular interest is the large increase which may be exhibited by the antenna conductance below the plasma frequency because of the finite electron temperature compared with the zero temperature conductance, for a given value of collision frequency.

I Introduction

There is currently a great deal of interest in the impedance characteristics of plasma-immersed antennas in connection with the possible exploitation of rocket and satellite borne antennas as probes to determine the ambient electrical properties of the ionosphere. The perturbing effect of the ionospheric plasma on the reactance of an electrically short antenna was reported on as early as 1952 by Jackson. A method was subsequently developed (Jackson and Kane, 1959, 1960; Kane et al 1962) that used a Q-meter type of observation for determining the electron density. Whale (1963) concluded that the resistive impedance component of the electrically short antenna in the ionosphere was also modified, due to radiating electron pressure waves as well as the usual electromagnetic (EM) wave, although his results must be viewed with some skeptism since he ignored electron collisions, which although infrequent in the ionosphere, may produce results which are by no means negligible, as will be shown below.

Further experimental probing of the ionosphere using radio frequency techniques has subsequently been reported on by Heikkila (1965a, 1965b), Heikkila et al (1966), Bramley (1965), MacKenzie and Sayers (1966 Stone, et al (1966a, 1966b) to mention only a few. The details of these various experiments differ. But they generally have in common an attempt to measure electron density from the change in reactance from free space of an rf driven electrode (antenna) or electrode pair immersed in the plasma.

A new and novel suggestion for measuring plasma electron densities was made by Takayama et al (1960). This scheme, called the plasma resonance probe, involves observing the dc current to a Langmuir

probe while a low level rf voltage is simultaneously applied to the probe and swept in frequency, the reported result being that a resonance in the dc probe current was observed as the rf frequency passed through the electron plasma frequency of the plasma outside the probe sheath. Further investigations carried out elsewhere conflicted with Takayama et al's results in that the resonance frequency appeared to consistently lie below the electron plasma frequency, being influenced by such factors as the sheath size, probe size and probe potential. It has since been accepted that the resonance does indeed lie below the electron plasma frequency; a discussion of both the theoretical and experimental aspects of the resonance probe is given by Harp and Crawford (1964).

A related area of investigation was begun by Field (1956) into the modifying effects of a finite electron temperature upon EM wave propagation in a plasma. He showed that the EM wave could couple to an electron pressure wave, or electrokinetic (EK) wave in regions of plasma inhomogeneity, sharp plasma boundaries, or as a result of static magnetic fields. Cohen (1962) later showed that the resistance of an electrically short current filament in a compressible (warm) plasma would be dominated by the effect of the finite temperature, with most of the energy being radiated in the EK mode. Many further investigations into the influence of the EK wave on the impedance of plasma immersed antennas have been carried out, including Balmain (1965), Hessel, et al (1962), Ament et al (1964), Seshadri (1965a, 1965b), Fejer (1964) and Wait (1964a, 1964b, 1965, 1966a). The conclusion reached as a result of these studies is generally that the EK wave may also be excited by a structure of finite dimension in the plasma (as

opposed to the filamentary current source of Cohen), but that the EK effect may be much reduced by a sheath, and as a consequence of the finite size of the antenna.

While the experimental evidence had not been at all conclusive regarding the relatively large effect on antenna impedance due to the EK wave predicted by such studies mentioned above, evidence of a different nature had been obtained that indicated the possible excitation of the EK wave by a plasma-immersed antenna. Resonance effects were observed during rocket tests of a topside sounder by Knecht et al (1961), the resonance phenomena appearing as echoes extending from the turnoff time of the sounder when the sounder frequency was equal to the electron plasma frequency, or the square root of the electron plasma frequency squared plus the electron cyclotron frequency squared (the upper hybrid frequency). Similar effects were observed on a second rocket flight (Knecht and Russel, 1962) and with the Alouette topside sounder (Lockwood, 1963), with additional resonances appearing at multiples of the electron gyrofrequency.

These resonances were explained by Calvert and Goe (1963) as being due to electrostatic oscillations excited in the vicinity of the antenna by the sounding pulse, with the energy partially fed back to the antenna when the pulse was turned off. More rigorous analyses of this phenomena were carried out by Fejer and Calvert (1964), Deering and Fejer (1965) and Dougherty and Monoghan (1966), the latter two incorporating the kinetic equations for the warm plasma rather than the fluid approach usually taken. These studies show that the observed resonances can be accounted for theoretically, and also predict some resonances not yet observed. The

resonances are studied by finding the singularities of the Fourier integrals for the space-time variations of the field of an infinitesimal current source dipole in the plasma. Deering and Fejer also obtained some expressions for the actual fields near the source, as a function of space and time.

This property of the plasma to resonate at characteristic frequencies after removing the excitation, has been called the relaxation resonance by Heikkela (1965a), to differentiate it from the resonance associated with the resonance probe. It appears that the relaxation resonance holds some promise for electron density measurements in the ionosphere, about which we will say more later.

We see that with the greater opportunities to observe the behavior of plasma-immersed antennas that have become available with the advent of rocket and satellite experimentation in the ionosphere, the picture of the antenna-plasma coupling has become more and more complex. From the earlier models where the plasma was characterized as a simple dielectric, the plasma is now recognized as a much more complicated medium, where it maybe unsafe to neglect any one aspect of the plasma properties without risk of omitting essential features of the physics involved. We see that in particular, the finite plasma temperature may produce gross variations from the dielectric plasma model, leading to sheath effects, radiation in an acoustical mode,and possibly enhancement of collisional effects because of the much shorter EK wavelength compared with the EM wavelength.

It is apparent that the analytical problem of dealing with the antenna immersed in a compressible, lossy, magnetoplasma is a very difficult one. It is only in the past few years that the problem of the linear antenna

more than a wavelength or so in length in free space can be said to have been numerically solved. And yet the same antenna when put into the plasma medium, leads to a problem of much greater complexity. Unlike the electrically short linear antenna in free-space, where both the dependence on length and the propagation constant of the antenna current may be reasonably approximated, this situation may not hold in the compressible plasma medium, since the EK wave may alter the antenna current. In addition, an electrically short antenna for EM waves may be very long for the EK wave. Also in contrast to the free-space situation, where a current filament may be used as a mathematical model of the real (thin) antenna, it appears from the work of Seshadri (1965a, 1965b) and Wait (1966a), that the finite transverse dimensions of the antenna and the presence of a sheath decrease the effect of the EK wave on the antenna impedance. Thus any results obtained from analyses using infinitesimal sources or assumed current distributions and neglecting the sheath must be viewed with some suspicion as giving undue importance to the effect of plasma compressibility.

There are two broadly different approaches one might consider using to more realistically analyze the impedance of the antenna in a warm magneto-plasma. One method would be an extension of that developed by Hallen (1930, 1938, 1939), King et al (1961) and others with an emphasis on the antenna current, which involves developing an integral equation (s) for the antenna current. The problem involves solving the integral equation, by no means an easy task, since for the compressible plasma, one obtains two coupled integral equations which lead to the current (Cohen, 1962). The other method involves formulating the problem as a boundary value problem,

with the emphasis on the antenna fields,. where an integral equation may arise involving the electric field in the antenna "aperture" (e.g., the cylindrical surface extending to infinity from the ends of a finite cylindrical antenna) or the electric field across the slot exciting the antenna. If the slot is thin compared with the wavelengths involved, then a good approximation in the later case is to assume a constant electric field across the slot, in which case the formal solution for the antenna current is obtained as a Fourier integral (or series). The former approach to antenna theory is essentially a circuit theory approach and the later a field theory approach (Schelkenoff, 1952). In either case, solving for the antenna impedance requires a "near field" solution, a generally much more difficult procedure than finding only the antenna radiation resistance, where only the far fields are required.

The method which is most appropriate to a given problem depends partly on the goemetry involved; in a case such as the infinite cylindrical antenna, there is no inherent difference between the two approaches, the formal results being identical. If the geometry of the antenna is such that its surface may be represented by a single coordinate in a particular coordinate system, then the boundary value approach is the natural one to use. On the other hand, the finite linear cylindrical antenna has been historically treated by the antenna-current integral equation approach, although Einarson (1966) has formulated this problem using the boundary value approach also.

Unfortunately however, if one desires to treat an antenna of finite size in a compressible plasma, and even then neglecting the static magnetic field, only in the case of spherical goemetry is the problem really tractable. As pointed out above, a pair of coupled integral equations result from the finite cylindrical antenna. The prolate spheroidal goemetry, an attractive

one for representing a finite, nearly cylindrical antenna with a single coordinate surface suffers from great computational difficulty if the plasma is lossy, (Wait, 1966b) and in addition shares with the biconical antenna analyzed by Schelkenoff (1952) the disadvantage of requiring the inversion of an infinite matrix for the solution. If the static magnetic field is added to the problem, then even the spherical geometry becomes impractical. However, the infinite cylindrical antenna can in principle be analyzed in this case, if the magnetic field is parallel to the cylinder axis. We thus choose to approach the investigation of the plasma-immersed antenna by treating the infinite cylindrical antenna, since it appears to offer the best possibility at present for making the fewest restrictive assumptions and including a maximum of the physical aspects of interest, while still being a practically solvable problem.

Our primary interest in this problem is in connection with the use of a linear dipole antenna, operated in a swept frequency mode in the ionosphere, for the purpose of exciting and detecting the relaxation resonance at the electron plasma frequency, to thus determine the ambient ionospheric electron density. The ultimate goal of our investigation would be to find the antenna current as a function of time so that the explicit effect of the relaxation resonance could be seen. This would require finding the antenna frequency response over a wide frequency range with a subsequent Fourier inversion from the frequency to the time domain. This is a very difficult computational problem, since even finding the impedance of the antenna at a single frequency is, as will be seen below, very involved. Consequently, we content ourselves in the present report to investigating only the frequency, and not the time, behavior, of the infinite antenna.

An analysis of the infinite cylindrical antenna is admittedly not as satisfying nor informative as a study of the finite antenna would be, but it appears to be definitely worthwhile pursuing, for the reasons mentioned above, and considering the intended application of the investigation. While the analysis cannot give, for example, absolute values for the impedance of the finite antenna, it can show the relative changes brought about by the various influencing factors such as plasma temperature, collision frequency, sheath parameters, etc. which may be expected to exhibit some of the same characteristics for the infinite antenna as for the finite antenna. Some care must be exercised here, since the free-space impedances of the infinite cylindrical antenna and the electrically short antenna, which must be taken into account if a reasonable comparison of the plasma perturbation on the impedance is to be made, may be considerably different; this will be discussed further below in presenting the results.

While the antenna is infinite, the source, which will be taken to be a circumferential slot of finite thickness with a specified voltage, is the same as used for the finite antenna. Thus the main difference between the two is that there are reflected waves on the finite antenna, which lead to resonance conditions with changing length that are not present on the infinite antenna, as well as to the impedance variation mentioned above.

The formulation of the problem is given in the next section, and is restricted for this report to the case of the compressible, lossy plasma, but without a static magnetic field. Section III contains a discussion of the numerical analysis used to obtain the numerical results which are given in section IV. The RMKS system of units will be used unless otherwise specified.

II Formulation

Our description of the field behavior in the plasma proceeds from the time-dependent hydrodynamic equations for the electrons (ion motion is neglected) together with Maxwell's equations, as

$$\left(\frac{\partial}{\partial t}+\underline{V}(\underline{r},t)\cdot\nabla\right)\underline{V}(\underline{r},t)=-\frac{q}{m}\underline{E}(\underline{r},t)-\nu\underline{V}(\underline{r},t) \qquad (1)$$
$$-\frac{\nabla P(\underline{r},t)}{mN(\underline{r},t)}-\frac{q}{m}\mu_o\underline{V}(\underline{r},t)\times\underline{H}(\underline{r},t)$$

$$\left(\frac{\partial}{\partial t}+\underline{V}(\underline{r},t)\cdot\nabla\right)N(\underline{r},t)+N(\underline{r},t)\nabla\cdot\underline{V}(\underline{r},t)=0 \qquad (2)$$

$$N(\underline{r},t)T^{-1/(\gamma-1)}(\underline{r},t)=\text{const} \qquad (3)$$

$$P(\underline{r},t)=kN(\underline{r},t)T(\underline{r},t) \qquad (4)$$

$$\nabla\times\underline{E}(\underline{r},t)=-\mu_o\frac{\partial}{\partial t}\underline{H}(\underline{r},t) \qquad (5)$$

$$\nabla\times\underline{H}(\underline{r},t)=\epsilon_o\frac{\partial}{\partial t}\underline{E}(\underline{r},t)-qN(\underline{r},t)\underline{V}(\underline{r},t) \qquad (6)$$

where $\underline{E}$ and $\underline{H}$ are the total electric and magnetic fields, V, N, P, and T are the macroscopic electron velocity, number density, pressure and temperature, -q and m are the electron charge and mass, ν is the electron collision frequency, γ the ratio of specific heats for the electron gas, $\underline{r}$ and t are the space and time coordinates, ϵ_o and μ_o are the permittivity and permeability of free space and k is Boltzmann's constant. Equation (1) is the momentum transport equation, (2) is the mass transport equation, (3) is the energy transport equation for adiabatic heat flow, (4) is the ideal gas equation of state and (5) and (6) are Maxwell's equations.

The usual method of dealing with Eqs. (1) - (6) is to linearize them, introducing time varying or dynamic perturbation quantities small in comparison with the non-time varying or static quantities. Since the resulting

boundary value problem will be dependent on the model used to account for the ion sheath, the two sheath models to be used in the analysis will be treated separately. In the vacuum sheath model, the actual sheath is replaced by a frespace layer, while in the inhomogeneous sheath model, the actual sheath inhomogeneity is included in the analysis. In either case, the sheath is assumed of finite thickness and of radius $\rho = s$, forming a concentric layer between the antenna surface of radius $\rho = c$, whose axis is coincident with the z-axis of the cylindrical (ρ, φ, z) coordinate system, and the external uniform plasma. The antenna is assumed to be excited by a circumferential slot of finite width δ, centered at $z=0$, across which voltage V_o is applied which is independent of azimuthal coordinate φ. As a result, there is no field variation in the φ direction and only an axial antenna current is excited. The present analysis is also to be restricted to the case of no static magnetic field.

II 1. The Vacuum Sheath.

A vacuum sheath has been used by Seshadri (1965b) and Wait (1966a) in connection with an antenna in a compressible plasma. In both cases, the analyses are restricted to a lossless plasma with the excitation frequency exceeding the electron plasma frequency. Larson (1966) recently studied the spherical dipole antenna, comparing the results for antenna admittance for both the vacuum and inhomogeneous sheath models, again for a lossless plasma with the excitation frequency above the electron plasma frequency. His results indicate that the vacuum sheath tends to exaggerate the influence of the EK wave compared with the more realistic inhomogeneous sheath.

These findings are substantially in agreement with those of Miller and Olte (1966a, 1966b), for the scattering of EM and EK waves from a plasma-immersed cylinder, where it was found that for EK wave incidence, the vacuum sheath model led to surface currents and scattering cross-sections approximately the same as those obtained from an inhomogeneous sheath about twice as thick. It appears then that the vacuum sheath model may be a reasonable first approximation of the actual inhomogeneous sheath, if its limitations are kept in mind.

Equations (1) - (6) are linearized by introducing the following variables,

$$\underline{E}(\underline{r}, t)=\underline{e}(\underline{r}, t) \tag{7a}$$

$$\underline{H}(\underline{r}, t)=\underline{h}(\underline{r}, t) \tag{7b}$$

$$\underline{V}(\underline{r}, t)=\underline{v}(\underline{r}, t) \tag{7c}$$

$$N(\underline{r}, t)=N+n(\underline{r}, t);\ |n| << N \tag{7d}$$

$$P(\underline{r}, t)=P+p(\underline{r}, t);\ |p| << P \tag{7e}$$

$$T(\underline{r}, t)=T+\tau(r, t);\ |\tau| << T \tag{7f}$$

since in the uniform plasma there is no static component of electric field or electron velocity. With the introduction of (7) into (1) - (6), we obtain

$$\nabla x\underline{e}(\underline{r}, t)=-\mu_o \frac{\partial}{\partial t}\underline{h}(\underline{r}, t) \tag{8}$$

$$\nabla x\underline{h}(\underline{r}, t)= \epsilon_o \frac{\partial}{\partial t}\underline{e}(\underline{r}, t)-qN\underline{v}(\underline{r}, t) \tag{9}$$

$$\frac{\partial}{\partial t}\underline{v}(\underline{r}, t)=-\frac{q}{m}\underline{e}(\underline{r}, t)-\nu\underline{v}(\underline{r}, t)-\frac{\gamma kT}{mN}\nabla n(\underline{r}, t) \tag{10}$$

$$\frac{\partial}{\partial t}n(\underline{r}, t)=N\ \nabla\cdot\underline{v}(\underline{r}, t)=0 \tag{11}$$

We will assign a value of 3 to γ, corresponding to adiabatic, one dimensional compression (Cohen 1962), so that Eq. (10) becomes

$$\frac{\partial}{\partial t}\underline{v}, (\underline{r}, t)=\frac{-q}{m}\underline{e}(\underline{r}, t)-\nu\underline{v}(\underline{r}, t)-\frac{v_r^2}{N}\nabla n(\underline{r}, t) \tag{10a}$$

where we have used $3kT=mv_r^2$ with v_r the rms electron velocity.

If we Fourier analyze the variables appearing in (8) - (11) by using

the Fourier transform pair

$$\underline{e}(\underline{r}, t)=\frac{1}{2\pi}\int_{-\infty}^{\infty} e^{i\omega t}\underline{e}(\underline{r}, \omega)d\omega$$

$$\underline{\tilde{e}}(\underline{r}, \omega)=\int_{-\infty}^{\infty} e^{-i\omega t}\underline{e}(\underline{r}, t)dt$$

then we get

$$\nabla x\underline{\tilde{e}}(\underline{r}, \omega)=-i\omega\mu_o\underline{\tilde{h}}(\underline{r}, \omega) \tag{12}$$

$$\nabla x\underline{\tilde{h}}(\underline{r}, \omega)=i\omega\epsilon_o\underline{\tilde{e}}(\underline{r}, \omega)-qN\underline{\tilde{v}}(\underline{r}, \omega) \tag{13}$$

$$(i\omega+\nu)\underline{\tilde{v}}(\underline{r}, \omega)=-\frac{q}{m}\underline{\tilde{e}}(\underline{r}, \omega)-\frac{v_r^2}{N}\nabla\tilde{n}(\underline{r}, \omega) \tag{14}$$

$$i\omega\tilde{n}(\underline{r}, \omega)+N\nabla\cdot\underline{\tilde{v}}(\underline{r}, \omega)=0 \tag{15}$$

We may now follow the usual technique for the spatially uniform plasma, by breaking the fields up into the EM and EK modes, with components denoted respectively by E and P, as

$$\nabla x\underline{\tilde{e}}_P=\nabla\cdot\underline{\tilde{e}}_E=0$$

with the well known result that

$$(\nabla^2+K_E^2)\underline{\tilde{h}}=0 \tag{16}$$

$$(\nabla^2+K_P^2)\tilde{n}=0 \tag{17}$$

where

$$K_E^2=K_{Eo}^2\epsilon_E$$

$$K_P^2=K_{Po}^2\epsilon_P$$

$$\epsilon_E=1-\frac{U^2}{(1-iV)}$$

$$\epsilon_P=1-U^2-iV$$

$$U=\omega_p/\omega=f_p/f$$

$$V=\nu/\omega=\nu/2\pi f$$

$$K_{Eo}=\omega/v_{\ell}$$

$$K_{Po}=\omega/v_{r}$$

with f_p the electron plasma frequency, and v_{ℓ} the free space propagation velocity of light. Since there is no azimuthal variation of the source or plasma and antenna structure, only the transverse magnetic (TM) ($H_z=0$) EM mode will be excited, along with the EK mode. The TM and EK field components are derivable from their corresponding scalar potentials $\tilde{\phi}_m^T$ and $\tilde{\phi}_p^T$ as

$$\tilde{\underline{e}}_m=\frac{1}{\bar{K}_E}\nabla x\nabla x(\hat{z}\tilde{\phi}_m^T)$$

$$\tilde{\underline{e}}_p=\nabla\tilde{\phi}_p^T$$

where now m and p are the subscripts used to denote the TM and EK mode field components and the T indicates the wave transmitted in the uniform plasma. The potentials $\tilde{\phi}_m^T$ and $\tilde{\phi}_p^T$ satisfy Eqs. (16) and (17) respectively, in terms of cylindrical Bessel functions involving the radial variable ρ, and an exponential z-direction variation with an exponent $i\beta$, β being the z-direction separation constant. Similarly, the EM fields in the vacuum sheath can be found from the potentials $\tilde{\phi}_m^I$ and $\tilde{\phi}_m^R$, which are solutions to (16) with $\omega_p=0.$, where the I and R denote the wave incident on the vacuum sheath-uniform plasma interface from the antenna, and that reflected back to the antenna from the sheath plasma interface.

A further Fourier analysis over β is required, since the source excites a continuous β spectrum of waves. We thus define the transform pair

$$\tilde{\underline{e}}(r,\omega)=\frac{1}{2\pi}\int_{-\infty}^{\infty}e^{i\beta z}\approx{\underline{e}}(\rho,\beta,\omega)d\beta$$

$$\approx{\underline{e}}(\rho,\beta,\omega)=\int_{-\infty}^{\infty}e^{-i\beta z}\tilde{\underline{e}}(\underline{r},\omega)dz$$

The spectral solutions $\tilde{\tilde{\phi}}_m^T$ and $\tilde{\tilde{\phi}}_p^T$ can now be written

$$\tilde{\tilde{\phi}}_m^T = A_m^T \; H_o^{(2)}(\lambda_E \rho) \tag{18}$$

$$\tilde{\tilde{\phi}}_p^T = A_p^T \; H_o^{(2)}(\lambda_P \rho) \tag{19}$$

with $H_o^{(2)}$ the cylindrical Hankel function of the second kind and order zero, and

$$\lambda_E^2 = K_E^2 - \beta^2$$

$$\lambda_P^2 = K_P^2 - \beta^2$$

where the -root of λ must be used to obtain the proper field behavior at infinity. In a similar fashion

$$\tilde{\tilde{\phi}}_m^I = A_m^I \; H_o^{(2)}(\lambda_{Eo} \rho) \tag{20}$$

$$\tilde{\tilde{\phi}}_m^R = A_m^R \; H_o^{(1)}(\lambda_{Eo} \rho) \tag{21}$$

where

$$\lambda_{Eo}^2 = K_{Eo}^2 - \beta^2$$

The specification of the problem is completed by introducing the boundary conditions to be satisfied by the fields at the sheath-plasma interface and the cylinder surface from which the A_-^- coefficients are to be obtained. These are continuity of the tangential magnetic and electric fields at the sheath-plasma interface, as well as the vanishing of the normal electron velocity there, thus assuming the sheath-plasma interface to elastically reflect the incident electrons. The latter boundary condition has received considerable criticism; it is an over simplification, but seems to be an approximation consistent with that of representing the actual sheath by the

vacuum sheath model. This question is discussed by Miller (1966) in further detail.

A last boundary condition is that the z-component (note that there is no φ -component of electric field) of the electric field vanish everywhere on the cylinder except at the slot, where it equals the excitation field,

$$-e_z(c,z,t)=V_o(t)/\delta;\ |z|<\delta/2$$
$$=0 \qquad |z|>\delta/2 \qquad (22)$$

where c is the cylinder radius. We would like to solve the problem $V_o(t)$ swept in frequency. This would require finding the antenna current as a function of frequency in order to perform the transform with respect to frequency. Thus for the present, with no loss of generality, we assume

$$V_o(t)=V_o e^{i\omega t};\ \text{all } t$$

so that

$$V_o(\omega)=V_o \delta(\omega-\omega') \quad 2\pi$$

where $\delta(\omega-\omega')$ is the delta function. The question of the antenna response to a source of finite time duration, and thus having a spectrum of frequencies will not be considered further in this report. We thus obtain the response of the antenna to the single excitation frequency $\omega=2\pi f$, and

$$-e_z(c,\beta,\omega)=V_o \delta(\omega-\omega') \ \frac{\sin(\beta\delta/2)}{(\beta\delta/2)} \ 2\pi \qquad (23)$$

is obtained. The boundary conditions may then be written in spectral form as

$$\begin{bmatrix} & & \\ & \triangle & \\ & & \end{bmatrix} \begin{bmatrix} A_m^I \\ A_m^R \\ A_m^T \\ A_p^T \end{bmatrix} = \begin{bmatrix} S(\beta) \\ 0 \\ 0 \\ 0 \end{bmatrix} \qquad (24)$$

where

$$\left[\Delta\right] = \begin{bmatrix} \frac{\lambda_{Eo}^2}{K_{Eo}} H_o^{(2)}(\lambda_{Eo}c); \frac{\lambda_{Eo}^2}{K_{Eo}} H_o^{(1)}(\lambda_{Eo}c); O; O \\ \frac{\lambda_{Eo}}{\eta_o} H_o^{(2)'}(\lambda_{Eo}s); \frac{\lambda_{Eo}}{\eta_o} H_o^{(1)'}(\lambda_{Eo}s); -\frac{\lambda_E}{\eta} H_o^{(2)'}(\lambda_E s); O \\ \frac{\lambda_{Eo}^2}{K_{Eo}} H_o^{(2)'}(\lambda_{Eo}s); \frac{\lambda_{Eo}^2}{K_{Eo}} H_o^{(1)}(\lambda_{Eo}s); -\frac{\lambda_E^2}{K_E} H_o^{(2)}(\lambda_E s); -i\beta H_o^{(2)}(\lambda_P s) \\ O; O; \frac{\lambda_E \beta}{K_E} H_o^{(2)'}(\lambda_E s); -\frac{i\lambda_P}{(1-\epsilon_E)} H_o^{(2)'}(\lambda_P s) \end{bmatrix}$$

$$S(\beta) = -V_o 2\pi \delta(\omega - \omega') \frac{\sin(\beta\delta/2)}{(\beta\delta/2)} \tag{25}$$

$$\eta = \frac{\omega\mu_o}{K_E}; \eta_o = \frac{\omega\mu_o}{K_{Eo}} \tag{26}$$

and c and s are the antenna and sheath radii and the prime indicates differentiation with respect to argument. A solution for the various coefficients A_-^- is straightforward, with the result

$$A_p^T = \frac{+i4\lambda_E\lambda_{Eo}^2\beta}{\pi s K_E K_{Eo}\eta_o} \frac{S(\beta)}{D} H_o^{(2)'}(\lambda_E s) \tag{27}$$

$$A_m^T = \frac{-4\lambda_P\lambda_{Eo}^2}{\pi(1-\epsilon_E)sK_{Eo}\eta_o} \frac{S(\beta)}{D} H_o^{(2)'}(\lambda_P s) \tag{28}$$

$$A_m^R = i\lambda_E\lambda_{Eo}\frac{S(\beta)}{D}\left[\frac{\lambda_P}{(1-\epsilon_E)} H_o^{(2)'}(\lambda_P s)\left(\frac{\lambda_{Eo}}{\eta K_{Eo}} H_o^{(2)}(\lambda_{Eo}s) H_o^{(2)'}(\lambda_E s)\right.\right.$$
$$\left.\left. -\frac{\lambda_E}{\eta_o K_E} H_o^{(2)}(\lambda_E s) H_o^{(2)'}(\lambda_{Eo}s)\right) \frac{\beta^2}{\eta_o K_E} H_o^{(2)}(\lambda_P s) H_o^{(2)'}(\lambda_E s) H_o^{(2)'}(\lambda_{Eo}s)\right] \tag{29}$$

$$A_m^I = \left[\frac{\bar{K}_{Eo}}{\lambda_{Eo}^2} S(\beta) - H_o^{(1)}(\lambda_{Eo}c) A_m^R\right] \frac{1}{H_o^2(\lambda_{Eo}c)} \tag{30}$$

where

$$D = -i \frac{\lambda_{Eo}^3 \lambda_E}{K_{Eo}} \left[\frac{W(c, s')}{\eta_o K_E} \left(\frac{\lambda_P \lambda_E}{(1 - \epsilon_E)} H_o^{(2)'}(\lambda_P s) H_o^{(2)}(\lambda_E s) \right.\right.$$

$$\left.\left. + \beta^2 H_o^{(2)}(\lambda_P s) H_o^{(2)'}(\lambda_E s) \right) - \frac{\lambda_P \lambda_{Eo} \eta^{-1}}{K_{Eo}(1 - \epsilon_E)} W(c, s) H_o^{(2)'}(\lambda_P s) H_o^{(2)'}(\lambda_E s) \right] \tag{31}$$

The Wronskian relations W(c, s) and W(c, s') are

$$W(c, s) = H_o^{(1)}(\lambda_{Eo}c) H_o^{(2)}(\lambda_{Eo}s) - H_o^{(1)}(\lambda_{Eo}s) H_o^{(2)}(\lambda_{Eo}c) \tag{32a}$$

$$W(c, s') = H_o^{(1)}(\lambda_{Eo}c) H_o^{(2)'}(\lambda_{Eo}s) - H_o^{(1)'}(\lambda_{Eo}s) H_o^{(2)}(\lambda_{Eo}c) \tag{32b}$$

The field quantities of interest are then obtained from their respective inverse Fourier transforms. In particular, the antenna current is obtained from

$$I(z, t) = 2\pi c h_\varphi (c, z, t) \tag{33}$$

$$= \frac{c}{2\pi} \int_{-\infty}^{\infty} e^{i\omega' t} e^{i\beta z} \approx h_\varphi (c, \beta, \omega') d\beta d\omega'$$

$$= -\frac{ci}{2\pi} \int_{-\infty}^{\infty} e^{i(\omega' t + \beta z)} \frac{\lambda_{Eo}}{\eta_o} \left[H_o^{(2)'}(\lambda_{Eo}c) A_m^I + H_o^{(1)'}(\lambda_{Eo}c) A_m^R \right] d\beta d\omega'$$

This can be simplified somewhat to give

$$I(z, t) = \frac{-2}{\pi^2 \eta_o} \int_{-\infty}^{\infty} \frac{e^{i(\omega' t + \beta z)}}{H_o^{(2)}(\lambda_{Eo}c)} \left[\frac{i\pi c K_{Eo}}{4\lambda_{Eo}} H_o^{(2)'}(\lambda_{Eo}c) S(\beta) - A_m^R \right] d\beta d\omega' \tag{34}$$

The ω' integration is readily performed, since the source is monochromatic, to give

$$I(z,t)=\frac{+V_o 4e^{i\omega t}}{\pi\eta_o}\int_{-\infty}^{\infty}\frac{e^{i\beta z}}{H_o^{(2)}(\lambda_{Eo}c)}\left[\frac{i\pi cK_{Eo}}{4\lambda_{Eo}}H_o^{(2)'}(\lambda_{Eo}c)\bar{S}(\beta)-\bar{A}_m^R\right]d\beta$$

$$=I(z,\omega)e^{i\omega t} \qquad (35)$$

where

$$\bar{S}(\beta)=\frac{\sin(\beta\delta/2)}{(\beta\delta/2)}$$

and $\bar{A}_m^R$ is given by Eq. (29) with $S(\beta)$ replaced by $\bar{S}(\beta)$. It is interesting to note that the first part of the integral in Eq. (35) is the free-space antenna current, which if we denote by $I_o(z,\omega)$, we can write

$$I_o(z,\omega)=\frac{+iV_o}{\eta_o}cK_{Eo}\int_{-\infty}^{\infty}e^{i\beta z}\frac{H_o^{(2)'}(\lambda_{Eo}c)}{H_o^{(2)}(\lambda_{Eo}c)}\frac{\bar{S}(\beta)}{\lambda_{Eo}}d\beta \qquad (36)$$

and $$I(z,\omega)-I_o(z,\omega)=\Delta I(z,\omega) \qquad (37)$$

with $$\Delta I(z,\omega)=\frac{-V_o}{\pi\eta_o}4\int_{-\infty}^{\infty}\frac{e^{i\beta t}\ \bar{A}_m^R}{H_o^{(2)}(\lambda_{Eo}c)}d\beta \qquad (38)$$

so that $\Delta I(z,\omega)$ gives the change in antenna current as a result of the plasma. We note that $\bar{A}_m^R \to 0$ in the limit $U\to 0$ and $\Delta I(z,\omega)$ becomes zero as required, if the plasma is removed.

The numerical evaluation of $I_o(z,\omega)$ has received considerable attention in the literature; attempts have also been made to obtain asymptotic expressions for the integral. It is easily shown that the real part of $I_o(z,\omega)$, which we denote I_{or}, has an integrable singularity at $\beta=K_{Eo}$(Duncan, 1962)

but that the imaginary part, I_{oi}, contains non-integrable singularities of opposite sign on either side of $\beta=K_{Eo}$. Further, the contribution to I_{or} comes entirely from the interval 0 to K_{Eo}. The presence of these singularities, particularly in I_{oi}, makes the numerical evaluation of I_o difficult, but not impossible; this is discussed in the next section.

It is also evident that the $\Delta I(z,\omega)$ integral has the same types of singularities as associated with I_o. This is shown quite readily from the small argument forms for the Hankel function; the details are shown in Appendix A. It is possible however to give an expression for $I(z,\omega)$ which does not have these non-integrable singularities. We do this by giving an alternative expression for A_m^I which is

$$A_m^I = i\lambda_E\lambda_{Eo}\frac{S(\beta)}{D}\left[\frac{-\lambda_P}{(1-\epsilon_E)}H_o^{(2)'}(\lambda_P s)\left(\frac{\lambda_{Eo}}{\eta K_{Eo}}H_o^{(1)}(\lambda_{Eo}s)H_o^{(2)'}(\lambda_E s)\right.\right.$$
$$\left.\left.-\frac{\lambda_E}{\eta_o K_E}H_o^{(1)'}(\lambda_{Eo}s)H_o^{(2)}(\lambda_E s)\right)+\frac{\beta^2}{\eta_o K_E}H_o^{(2)}(\lambda_P s)H^{(1)'}(\lambda_{Eo}s)H_o^{(2)'}(\lambda_E s)\right] \quad (30a)$$

If we insert this expression into Eq. (33) along with (29) for A_m^R and integrate over ω', we obtain

$$I(z,\omega)=\frac{+icV_o}{\eta_o}\int_{-\infty}^{\infty} e^{i\beta z}\,\bar{S}(\beta)\frac{A}{D}\lambda_{Eo}^2\,d\beta$$
$$=\int_0^{\infty} I(\beta,\omega)\cos(\beta z)\sin(\beta\delta/2)\,d\beta \quad (39)$$

where

$$A=\lambda_E\left[\frac{W(c',s')}{\eta_o K_E}\left(\frac{\lambda_P\lambda_E}{(1-\epsilon_E)}H_o^{(2)'}(\lambda_P s)H_o^{(2)}(\lambda_E s)\right.\right.$$
$$\left.\left.+\beta^2 H_o^{(2)}(\lambda_P s)H_o^{(2)'}(\lambda_E s)\right)-\frac{\lambda_P\lambda_{Eo}}{(1-\epsilon_E)}\frac{W(c',s)}{K_{Eo}\eta}H_o^{(2)'}(\lambda_P s)H^{(2)'}(\lambda_E s)\right]/i \quad (40a)$$

$$I(\beta,\omega)=\frac{+2ic V_o}{\eta_o}\lambda_{Eo}^2\ \frac{A}{D}\ \frac{1}{(\beta\delta/2)} \tag{40b}$$

and

$$W(c',s)=H_o^{(1)'}(\lambda_{Eo}c)H_o^{(2)}(\lambda_{Eo}s)-H_o^{(1)}(\lambda_{Eo}s)H_o^{(2)'}(\lambda_{Eo}c) \tag{32c}$$

$$W(c',s')=H_o^{(1)'}(\lambda_{Eo}c)H_o^{(2)'}(\lambda_{Eo}s)-H_o^{(1)'}(\lambda_{Eo}s)H_o^{(2)'}(\lambda_{Eo}c) \tag{32d}$$

It may be verified (as shown in Appendix A) that (39) contains no non-integrable singularities as long as the electron collision frequency is non-zero. In the event that $\nu=0$, singularities determined by K_E, K_P and s-c do occur. These singularities are discussed by Seshadri (1965b). Consequently, the introduction of electron collisions in the formulation makes the problem numerically more tractable as well as physically more realistic.

We can finally obtain the antenna admittance Y by finding the current at $z=\delta/2$, and forming the ratio*

$$\frac{I(\delta/2,\omega)}{V_o}=Y(\omega)=G(\omega)+jB(\omega) \tag{41}$$

This is the quantity of most interest to us in this investigation, and for which we will present the most extensive numerical results. During the evaluation of the integral for $Y(\omega)$, we can also evaluate the other Fourier coefficients (27) and (28) from which the field quantities of interest may be obtained by inverting the corresponding Fourier integrals. We could for example, examine the power flow in the plasma in the EM and EK waves as a function of ρ and z. Information of this type should provide some idea of the primary interaction volume of the antenna with the plasma, from which we may deduce the effective antenna sampling volume in relation to the antenna's use as a probe to determine

* Note that $B(\omega)$ is finite only for non-zero δ.

the ambient plasma properties. It is also of interest to find the antenna current as a function of z, particularly since a decreasing current magnitude with increasing z may give an order of magnitude indication of the length of a finite antenna beyond which its impedance may differ negligibly from that of the infinite antenna. This is because the importance of current reflections from the end of the finite antenna becomes less with decreasing current magnitude. Since our primary interest in the present report is the antenna admittance, we will defer a detailed study of the antenna near fields to a subsequent report, wherethis question, along with the relaxation resonance problem, will be considered. Since the numerical technique of inverting the nearly singular Fourier integrals which occur in this formulation is of great importance if the analysis is to be carried further, section III of this report will briefly describe the procedure used.

II. 2 The Inhomogeneous Sheath

The same set of linearized equations is used to obtain the fields in the uniform plasma for the inhomogeneous sheath model as for the vacuum sheath model i.e., Eqns. (1) - (6). For the sheath itself however, the linearized set of variables given by (7) contains in addition a static component of electron velocity and electric field. In the present study, where we take the antenna to be at floating potential, it may be shown to be a reasonable approximation to neglect the static electron velocity (see Miller, 1966), which is what we do here, so that (7) is the same except for (7a) which becomes

$$\underline{E}\ (\underline{r}, t)=\underline{E}(\underline{r}\ )\ +\underline{e}(\underline{r}, t); \qquad |e\ | << E \tag{7a)'}$$

and N and P are now functions of $\underline{r}$.

The linearized equations (8) - (11) are unchanged except for (10a) which is now

$$\frac{\partial}{\partial t}\underline{v}(\underline{r}, t)=-\frac{q}{m}\left(\underline{e}(\underline{r}, t)+\underline{E}(\underline{r})\frac{n(\underline{r}, t)}{N(\underline{r})}\right)$$

$$-\nu\underline{v}(\underline{r}, t)-\frac{v_r^2}{N(r)}\nabla\underline{n}(\underline{r}, t) \qquad (10a)'$$

After the Fourier transformation is applied, Eq. (10a)' becomes

$$(i\omega+\nu)\tilde{\underline{v}}(\underline{r}, \omega)=-\frac{q}{m}\left(\tilde{\underline{e}}(\underline{r}, \omega)+\frac{E(\underline{r})}{N(\underline{r})}\tilde{n}(\underline{r}, \omega)\right) \qquad (14a)'$$

$$-\frac{v_r^2}{N(\underline{r})}\nabla\tilde{n}(\underline{r}, \omega)$$

with the other equations as given by (12), (13) and (15).

The presence of the term containing $\underline{E}(\underline{r})/N(\underline{r})$ in (14a)' prevents us from decomposing the total electric field into EM and EK components as for the uniform plasma. This is most readily seen by writing an expression for $\tilde{\underline{e}}(\underline{r}, \omega)$ as

$$\tilde{\underline{e}}(\underline{r}, \omega)=\frac{1}{i\omega\epsilon_o\epsilon_E}\left[\nabla x\tilde{\underline{h}}(\underline{r}, \omega)+\nabla\tilde{p}(\underline{r}, \omega)+\underline{L}(\underline{r})\tilde{p}(\underline{r}, \omega)\right] \qquad (42)$$

where

$$\tilde{p}(\underline{r}, \omega)=\frac{qv_r^2\tilde{n}(\underline{r}, \omega)}{i\omega(1-i\nu)}$$

$$\underline{L}(\underline{r})=\frac{e}{mv_r^2}\underline{E}(\underline{r})$$

We see that $\nabla x\tilde{\underline{e}}(\underline{r}, \omega)$ and $\nabla\cdot\tilde{\underline{e}}(\underline{r}, \omega)$ will contain terms in both $\tilde{\underline{h}}(\underline{r}, \omega)$ and $\tilde{p}(\underline{r}, \omega)$, in contrast to the uniform plasma case where $\underline{L}(\underline{r})=0$, with the result that the magnetic field and dynamic electron density are coupled. Two coupled

wave equations similar to (16) and (17) may be obtained as

$$(\nabla^2+K_E^2)\tilde{\underline{h}}+\underline{P}x\nabla x\tilde{\underline{h}}=\nabla\tilde{p}x(\underline{P}+\underline{L}) \tag{43}$$

$$(\nabla^2+K_P^2)\tilde{p}+\nabla\cdot(\underline{L}\tilde{p})-\underline{P}\cdot(\underline{L}\tilde{p}+\nabla\tilde{p})=\underline{P}\cdot\nabla x\tilde{\underline{h}} \tag{44}$$

where

$$\underline{P}=\frac{\nabla\epsilon_E}{\epsilon_E}$$

If the plasma is uniform, then $\underline{P}=\underline{L}=0$ and (43) and (44) reduce to (16) and (17). The inhomogeneous sheath is specified for our purposes, by the static potential variation in the sheath. We take the static potential ϕ_o to vary as

$$\phi_o=\phi_c\left[\frac{s-\rho}{s-c}\right]^M \tag{45a}$$

where ϕ_c is the cylinder potential, and M is an adjustable parameter. We obtain ϕ_c from a form due to Self (1963) as

$$\phi_c=\frac{-kT}{e}\log_e\left[\sqrt{\frac{m_i}{m}}\frac{1}{1.22}\right] \tag{45b}$$

where m_i is the ion mass. The static electric field is then obtained as

$$\underline{E}(\underline{r})=-\nabla\phi_o$$

while $N(\underline{r})$ is given by

$$N(\underline{r})=N_\infty\exp\left[e\phi_o/kT\right]$$

with N_∞ the electron density in the uniform plasma. A more complete discussion of the applicability of this description for the static sheath is given by Miller (1966).

The first order differential equations corresponding to (43) and (44) are more convenient to use in the numerical solution which is required, and are, after a Fourier transform with respect to z,

$$\tilde{\tilde{p}}' = (i\omega\epsilon_o\epsilon_E)\tilde{\tilde{e}}_\rho + i\beta\tilde{\tilde{h}}_\varphi - L\tilde{\tilde{p}}$$

$$\tilde{\tilde{h}}_\varphi' = -\frac{\tilde{\tilde{h}}_\varphi}{\rho} + (i\omega\epsilon_o\epsilon_E)\tilde{\tilde{e}}_z - i\beta\tilde{\tilde{p}}$$

$$\tilde{\tilde{e}}_z' = -i\beta\tilde{\tilde{e}}_z - \frac{\tilde{\tilde{e}}_\rho}{\rho} + \frac{i\omega(1-iV)}{\epsilon_o v_r^2}\tilde{\tilde{p}}$$

$$\tilde{\tilde{e}}_z' = i\omega\mu_o\tilde{\tilde{h}}_\varphi + i\beta\tilde{\tilde{e}}_\rho$$

where the ' denotes differentiation with respect to ρ.

As for the vacuum sheath model, the fields in the uniform plasma are derivable from scalar potentials involving unknown Fourier constants to be determined from the boundary conditions. The total number of integration constants to be determined is 6; 4 for the sheath fields and 2 for the transmitted fields in the uniform plasma. The boundary conditions which are used here are continuity of the tangential electric and magnetic fields, the normal fluid velocity and the dynamic electron number density at the sheath-uniform plasma interface (ρ=s). At the antenna surface (ρ=c), we require the z-component of the electric field to be zero everywhere except at the slot, where it equals the excitation field as before, and we use an admittance relation between the normal electron velocity and dynamic electron number density (see Cohen, 1962), given by

$$\hat{\rho}\cdot\underline{v} = Y_B n \qquad (50)$$

The boundary condition equations can be written then, after eliminating the Fourier coefficients of the transmitted fields in the uniform plasma, as:

ρ = c:

$$i\omega\epsilon_o\tilde{\tilde{e}}_\rho + i\beta\tilde{\tilde{h}}_\varphi = -\frac{i\omega(1-iV)}{v_r^2}NY_B\tilde{\tilde{p}} \qquad (51a)$$

$$\tilde{\tilde{e}}_z = -V_o \frac{\sin(\beta\delta/2)}{(\beta\delta/2)}\delta(\omega-\omega')\,2\pi \qquad (51b)$$

$\rho = s$:

$$\approx_1 \tilde{\tilde{h}}_\varphi + \frac{h_\varphi}{\rho} + \lambda_E^2 \frac{H_o^{(2)}(\lambda_E s)}{H_o^{(2)}(\lambda_E s)} \approx h_\varphi = 0 \qquad (52a)$$

$$\approx_1 p - \frac{H_o^{(2)}(\lambda_P s)}{H_o^{(2)}(\lambda_P s)} \approx p = 0 \qquad (52b)$$

The surface current on the antenna is found from

$$I_z(z,t) = 2\pi c h_\varphi(c,z,t)$$

$$= e^{i\omega t} c \int_{-\infty}^{\infty} e^{i\beta z} \bar{h}_\varphi(c,\beta,\omega) d\beta$$

$$= I_z(z,\omega) e^{i\omega t} \qquad (53)$$

where

$$\tilde{\tilde{h}}_\varphi(c,\beta,\omega) = 2\pi\, \delta(\omega - \omega') \bar{h}_\varphi(c,\beta,\omega)$$

for a monochromatic source of frequency ω.

While the solution for the antenna admittance follows formally for the inhomogeneous sheath in the same manner as for the vacuum sheath, there is one important difference. The integrand function for the vacuum sheath is straightforward to evaluate, involving an analytic expression containing functions which are readily (and rapidly) calculated. For the inhomogeneous sheath however, evaluation of the integrand function requires the numerical solution of 4 coupled, complex, first order differential equations across the sheath region, a process which by comparison, is much more time consuming than for the vacuum sheath. In addition the numerical solution of a boundary value problem when the boundary conditions are expressed at two boundaries such as we have here, is straightforward, but more time consuming than for the initial value problem, where the boundary conditions are all given at the same location. This is an additional factor to consider in obtaining a solution for the inhomogeneous sheath problem.

Consequently, while a solution should be obtainable in principle, the practical aspect of the expense involved may deter us from obtaining numerical results. The inhomogeneous sheath analysis is included here for the sake of completeness, but no calculations pertaining to the inhomogeneous sheath are included in this report.

III. Numerical Analysis

There are many standard methods for the numerical evaluation of definite integrals, which fall in the category known as numerical quadrature. Numerical quadrature is the process of approximating an integrand piecewise by polynomials and integrating these exactly. One example of a quadrature scheme is Gaussian quadrature, of which there are many types, depending on the weight function which may be factored from the integrand function. A characteristic of Gaussian quadrature is that the abscissa points are typically determined by the zeroes of some type of polynomial, and as a result are not equally spaced. This is a great disadvantage in integrating functions which are complicated, and consequently time consuming to evaluate, as in our case, since in any iteration procedure or change of interval size to improve the accuracy, it is desirable to utilize previously calculated integrand values.

A different class of quadrature formulas based on equally spaced abscissa points, is the Newton-Cotes method, special cases of which are the well-known Trapezoidal rule for the order 1 and Simpson's rule (also called the parabolic rule) for the order 2. A particularly useful method for applying the Trapezoidal rule, called Romberg integration, employs Richardson's deferred approach to the limit (Ralston, 1965, p. 118). This is a technique whereby two approximate results are combined in a certain way to get a third and hopefully better result. The technique is used in Romberg's integration by calculating two values, using the Trapezoidal rule, for an integral over a fixed interval, the second value being obtained using twice the number of subintervals as employed for the first. Following Ralston,

we denote these quantities by T_{0k} where

$$T_{0k} = \frac{b-a}{2^k}\left(0.5\, f_0 + f_1 + f_2 + \ldots + f_{2^k-1} + 0.5\, f_{2k}\right) \tag{54}$$

and the integral whose value we desire is

$$J = \int_a^b f(x)dx$$

$$f_n = f(a+nh); n=0, 1, \ldots, 2^k$$

$$h = \frac{b-a}{2^k}$$

We see that the quantities $T_{0,k}$; k=0, 1, . . . are successive Trapezoidal approximations to J.

We then define, using Richardson's deferred approach to the limit,

$$T_{1,k} = \frac{1}{3}\left(4\, T_{0,k+1} - T_{0,k}\right); k=0, 1, \ldots \tag{55a}$$

which upon using (54) can be shown to reduce to Simpson's rule. This can be made more general by writing

$$T_{m,k} = \frac{1}{4^m - 1}\left(4^m T_{m-1,k+1} - T_{m-1,k}\right) \tag{55b}$$

$$m=1, 2, \ldots$$

$$k=0, 1, \ldots$$

The approximation $T_{2,k}$ is the composite Newton-Cotes rule of order 4 with 2^k subintervals, but for m>2 there is no direct relation between $T_{m,k}$ and a Newton-Cotes composite rule (Ralston, 1965). The Romberg integration answer is given by $T_{m,0}$.

The utility of the Romberg integration scheme may be seen by observing that Simpson's rule is a generally more accurate integration technique than the Trapezoidal rule, for the same number of abscissa points. Ralston presents an example, the integration of $\int_1^3 dx/x$, for which Simpson's rule gives 7 place accuracy (1 unit off in the seventh significant figure) with 33 abscissa points, whereas the Trapezoidal rule gives only 6 place accuracy (2 units off in the sixth figure) with 129 absicssa points. Romberg integration on the other hand, gives 7 place accuracy with only 17 abscissa points, from $T_{4,0}$.

Along with its generally greater accuracy, Romberg integration has another very attractive advantage in that the convergence of the successively calculated $T_{m,0}$ values provides a built-in testing procedure for estimating the error arising in each integration interval (a, b). In practice, it is convenient to arrange the $T_{m,k}$ in a triangular array, as follows:

$$
\begin{array}{ccccccc}
T_{0,0} & & & & & & \\
T_{0,1} & T_{1,0} & & & & & \\
T_{0,2} & T_{1,1} & T_{2,0} & & & & \\
\vdots & \vdots & \vdots & & & & \\
\vdots & \vdots & \vdots & \ddots & & & \\
\vdots & \vdots & \vdots & \ddots & \ddots & & \\
T_{0,m} & T_{1,m-1} & \cdots & \cdots & \ddots & T_{m,0} &
\end{array}
$$

The first column thus gives the Trapezoidal rule answers, while the second gives answers obtained from Simpson's rule, and the diagonal gives the Romberg answers. Convergence towards the correct result occurs along

the diagonal and down the left hand column. In addition, the answers converge towards $T_{m,0}$ along each row, and generally the row convergence gives an earlier indication of convergence to a desired accuracy than does the diagonal. The T-array for the example mentioned above is (Ralston, 1965, p. 125)

m	$T_{0,m}$					
0	1.333333					
1	1.166667	1.111111				
2	1.116667	1.10000	1.099259			
3	1.103211	1.098726	1.098641	1.098631		
4	1.099768	1.098620	1.098613	1.098613	1.098613	
5	1.098902	1.098613	1.098613	1.098613	1.098613	1.098613
6	1.098685	1.098613	1.098613	.	.	.
7	1.098630	1.098612	1.098612	.	.	.

The answer, correct to 7 figures is 1.098612.

The superiority of the Romberg method is very evident in this example. Care must be taken in its application however, as the $T_{m,0}$ may oscillate widely about the correct answer and actually require more abscissa points than the $T_{0,m}$ values to obtain a desired accuracy, for functions having a sharp maxima (or minima) in the interval (a, b). In this case then, the row convergence can not be relied upon to indicate the accuracy of a given $T_{m,0}$. An additional drawback in this situation is that, since the abscissa points are evenly distributed within the interval (a, b), many more points are obtained outside the maxima (minima) than required in order to get the necessary abscissa spacing with the maxima (minima). Thus, the Romberg method is very powerful in the integration of monotonically varying functions,

but has some limitations where peaked functions are concerned if the integration interval is wider than the peak. In the following, the application of the Romberg integration scheme to our specific problem is briefly discussed.

It should be noted that while the Romberg answer $T_{m,0}$ can be obtained by generating the T-array discussed above, an answer can also be obtained in the more usual way, as

$$T_{m,k}=h \sum_{j=0}^{2^{m+k}}{}' d_{jm} f(a+jh) \tag{56}$$

where

$$h=\frac{b-a}{2^{m+k}}$$

The d_{jm} weights are obtained as (Bauer, et al., 1963),

$$d_{jm}=c_{m0}+2c_{m1}+4c_{m2}+\ldots+2^{p}c_{mp} \tag{57a}$$

with p the highest power of 2 by which j is exactly divisible (i.e., for j odd, p=0) and

$$c_{0,0}=1 \tag{57b}$$

$$c_{mk}=\frac{(-1)^{k}c_{m-k,0}}{3\cdot 15\cdot 63\cdots(4^{k}-1)} \quad ; \quad k=1,1,\ldots m \tag{57c}$$

$$c_{m,0}=1-\sum_{j=1}^{m} c_{mj} \tag{57d}$$

The prime on $\sum$ in (56) indicates the end points are to be taken with one half the weight.

Obviously, the abscissa points to be used are required before the application of (56). The utility of this expression for the integral comes in the situation of interest in this report, where the values of several integrals may be desired. If the integrals have similar variation with the integration variable, then the convergence test, with its attendant time and storage requirements, can be performed for one of the integrals, the others being obtained from (56).

The problem facing us is that of evaluating an integral over the range 0 to ∞. We obviously can not carry out the integration numerically over this range, and consequently seek to determine some finite upper limit beyond which the truncation error arising from the neglected portion of the integral is smaller than an acceptable relative truncation error, E_T. We mention again, as was earlier pointed out, that the integral (39) is convergent only if the feeding gap thickness δ, is non-zero. In order to establish the truncation error, we write the current, following (39), as

$$I(z,\omega)=I_A+I_B \tag{58a}$$

where

$$I_A=\int_0^B I(\beta,\omega)\cos(\beta z)\sin(\beta\delta/2)d\beta \tag{58b}$$

$$I_B=\int_B^\infty I(\beta,\omega)\cos(\beta z)\sin(\beta\delta/2)dd\beta \tag{58c}$$

and we seek to find a value for B where the truncation error, due to neglecting the contribution of I_B to $I(z,\omega)$, is less than E_T. It may be shown that as $\beta\rightarrow\infty$, $I(\beta,\omega)\rightarrow\beta^{-2}$ from the large argument expressions for the Hankel functions. We can then write

$$I_B \cong B^2 I(B,\omega) \int \frac{\cos(\beta z)\sin(\beta \delta/2)\,d\beta}{\beta^2} \qquad (59)$$

with

$$I(B,\omega) = I(\beta,\omega)\Big|_{\beta=B}$$

now

$$|I_B| \leqslant |B^2 \; I(B,\omega)| \int_B^\infty \left| \frac{\cos(\beta z)\sin(\beta \delta/2)\,d}{\beta^2} \right| \qquad (60)$$

$$\leqslant B^2 \; |I(B,\omega)| \int_B^\infty \frac{d\beta}{\beta^2}$$

$$= B \; |I(B,\omega)|$$

Since we want $\left|\frac{I_B}{I_A}\right| \leqslant E_T$

we get

$$\frac{B\,|I(B,\omega)|}{|I_A|} \leqslant E_T \qquad (60$$

The integration of (39) was terminated wherever (60) was satisfied, with B equal to the current value of β.

Still required is a means of choosing the optimum interval size for applying the Romberg integration. Obviously, the optimum interval size is the one which yields the highest accuracy with the fewest abscissa points. Since the near-singularities of the function being integrated are not a priori known in either location or width, the only reliable way for choosing the interval size is to have this done by the computer in the course of the calculations. The manner by which this was accomplished is briefly as follows.

The integration is begun at $\beta = 0$, with some initial specified interval width w_1 ($a_1 = 0$, $b_1 = a_1 + w_1$). The integrand is evaluated, successively, at $\beta = a_1$ and $\beta = a_1 + w_1$, and the first entry in the T array for that interval is calculated. A third absicssa point, at $\beta = a_1 + w_1/2$, is then calculated, so that the second row of the T-array may be obtained. A convergence test is then performed, which requires that

$$\left|(T_{1,0} - T_{0,1})/T_{1,0}\right| \leqslant E_C \tag{61a}$$

where E_C is maximum acceptable convergence error. The failure of this test leads to two new abscissa points, at $\beta = a_1 + w_1/4$ and $\beta = a_1 + 3w_1/4$ and the generation of the third row of the T-array. The convergence test then requires that

$$\left|(T_{2,0} - T_{1,1})/T_{2,0}\right| \leqslant E_C \tag{61b}$$

Failure of this test could lead to still finer subdivisions of the (a_1, b_1) interval, until a convergence test of the form

$$\left|(T_{m,0} - T_{m-1,1})/T_{m,0}\right| \leqslant E_C$$

is satisfied. It should be observed that we are employing a row convergence test, rather than a diagonal test, since as mentioned above, it was found that row convergence gave an earlier indication of acceptable accuracy than did the diagonal.

As was mentioned previously, this procedure is generally not desirable, since the bracketing of a sharp maxima by the interval (a_1, b_1) results in an

oscillating Romberg answer with slow convergence to the correct result, as well as an excessive number of abscissa points, outside the maxima. Instead, if convergence is not obtained from a maximum of 5 abscissa points in the interval (i.e., $m \leqslant 2$), the interval is divided in two, and a T-array calculated for the first of these two new intervals, $(a_1, a_1+w_1/2)$, from the 3 abscissa points already obtained. Failure of the convergence test here leads to the calculation of 2 additional abscissa points for this new interval $(a_1, a_1 + w_1/2)$. If convergence is still not obtained, two new intervals are formed from $(a_1, a_1 + w_1/2)$, with this general procedure being continued until the desired convergence is established. On the other hand, if convergence had been obtained on (a_1, b_1) with $m \leqslant 2$, then the interval width $w_2=2w_1$ is used for the next interval (a_2, b_2). We point out that 5 abscissa points are allowed per interval, rather than only 3, since the failure of convergence with 3 points would then require 5 points to be obtained anyway if the interval is then halved, because 3 abscissa points are required for each of the two new intervals to test the convergence.

We thus obtain a sequence of intervals of width such that the desired convergence occurs on each interval with no less than 3 and no more than 5 abscissa points being used. Note that the end points of the intervals are used twice, once for each adjacent interval. The convergence error, E_C, is adjusted during the calculations to keep the absolute error arising from each interval below an acceptable level relative to the largest contribution of the preceding intervals. The reason for this is to avoid unnecessary calculations which do not increase the accuracy of the integration. For example, if the contribution to the integration of interval i is C_i and the

largest contribution of the preceding i-1 intervals is C_{i-j} at interval i-j, and $C_i \approx 10^{-y} C_{i-j}$ with $y > 1$, then $C_i + C_{i-j} \approx (1+10^{-y})C_{i-j}$. Thus, if C_{i-j} has a normalized accuracy no less than E_C, there is no need to know C_i to a normalized accuracy better than $10^y E_C$. In essence, we attempt to maintain the same absolute accuracy in each interval of the integration. The advantage of doing this is shown in Appendix B.

In practice, the real and imaginary parts of the current were tested separately for convergence. It was found that this computation scheme consistently chose the smallest interval size at the location of maxima in the integrand, which is the desired result. The ratio of the largest to the smallest abscissa spacing was found to be as large as 10^6 to 10^7. An interesting aspect of the method is that, in the region of largest contribution to the integral, the contribution from the successive intervals were generally on the same order of mangitude, which is desirable from the error analysis. It should be noted that if the abscissa spacing becomes too small relative to the current value of β, it may be necessary to use double precision calculations, if the change in β is smaller than the least significant figure available in the computer.

When other quantities are desired in addition to the slot current, the necessary integrand values $f(a_i+jh)$ may be stored, and the computation performed using

$$F = \sum_{i=1}^{N} f_i \tag{62a}$$

$$f_i = h \sum_{j=0}^{2^{m+k}}{}' d_{jm} f(a_i+jh) \tag{62b}$$

where h and d_{jm} are given by (56) and (57a), and a_i is the initial abscissa point for each i'th interval with N the total number of intervals. In order to save time retrieving the quantities required, these were stored sequentially as calculated, and an index number used to locate them in storage as the summation (62) is performed. A copy of the program may be obtained from the author.

IV. Numerical Results

IV. 1 Free Space Admittance

It has been shown previously, that the antenna current (and admittance) can be expressed as the sum of two components, one being that for the case where the antenna is located in free space, and the other arising from the effect of the plasma. The relative change from the free space value of the antenna admittance brought about by the plasma is of interest, requiring a consideration of the free space admittance values. Since the expression for the free space admittance contains non-integrable singularities on the real β-axis, the problem of numerically obtaining the free-space admittance is not straight forward.

A number of papers have appeared rather recently on the free-space admittance of the infinite cylindrical antenna. Duncan (1962) examined the problem in some detail, outlining a computation scheme for obtaining numerical admittance values which involves a series approximation to the exact integral. He gives some admittance values for $K=K_{Eo}c$ ranging from 0.01 to 0.15, but since he uses a delta function gap and performs an averaging process in the vicinity of the gap, his susceptance values are of questionable value, though the conductance values can be used since the conductance is independent of the gap thickness.

Chen and Keller (1962) and Fante (1966) attempt to derive analytic forms of the admittance by using approximate expressions for the Hankel functions for various ranges of the β-integration. Both of these papers contain errors, those of Chen and Keller being pointed out by Fante, while Fante's errors are shown by Miller (1967). These attempts

to give a closed form for the free space admittance are useful in providing a rough approximation to the exact values and the influence of the various parameters involved, but the results are not accurate enough for our purpose.

Instead of approximating the integrand in order to obtain numerical free space admittance values as was done in the papers quoted, we have chosen to deform the contour in integrating the exact expression for the current, given by (36). This is most easily done numerically, by integrating upward, along the positive imaginary β -axis, and then proceeding at right angles parallel to the positive real β-axis, until the truncation error is acceptably small. The coutour can be brought downward to the real β -axis once the singularity at $\beta = K_{Eo}$ has been passed, but the contribution to the integral of this segment may be neglected if the path parallel to the real axis is carried far enough to obtain the small truncation error desirable. The contour used for obtaining the free space admittance is shown in Fig. 1.

We present in Fig. 2 the free space admittance for an antenna 1 cm in radius, and various gap thicknesses δ, as a function of frequency between 300 KHz and 10 MHz. This antenna radius and frequency range is chosen to correspond to the values expected to apply to a projected experiment in the ionosphere.

We observe that the conductance and susceptance show a rather slow increase with increasing frequency, and that the conductance exceeds the susceptance over the entire range, Further, the susceptance is not sensitive to changing gap thickness, for this frequency range, though

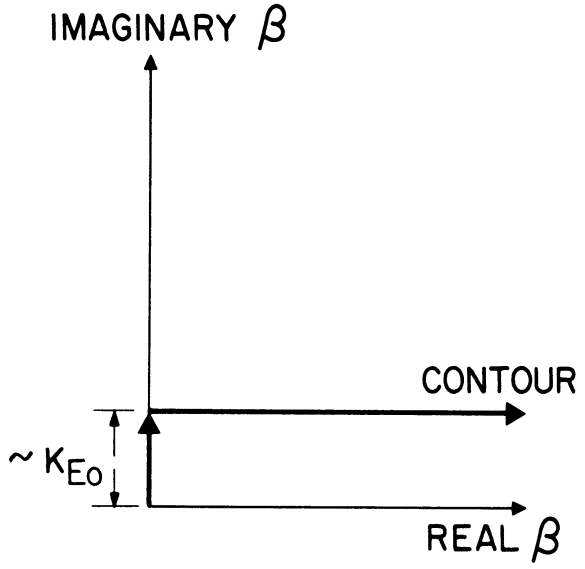

Fig. 1. Integration contour for obtaining the free-space admittance.

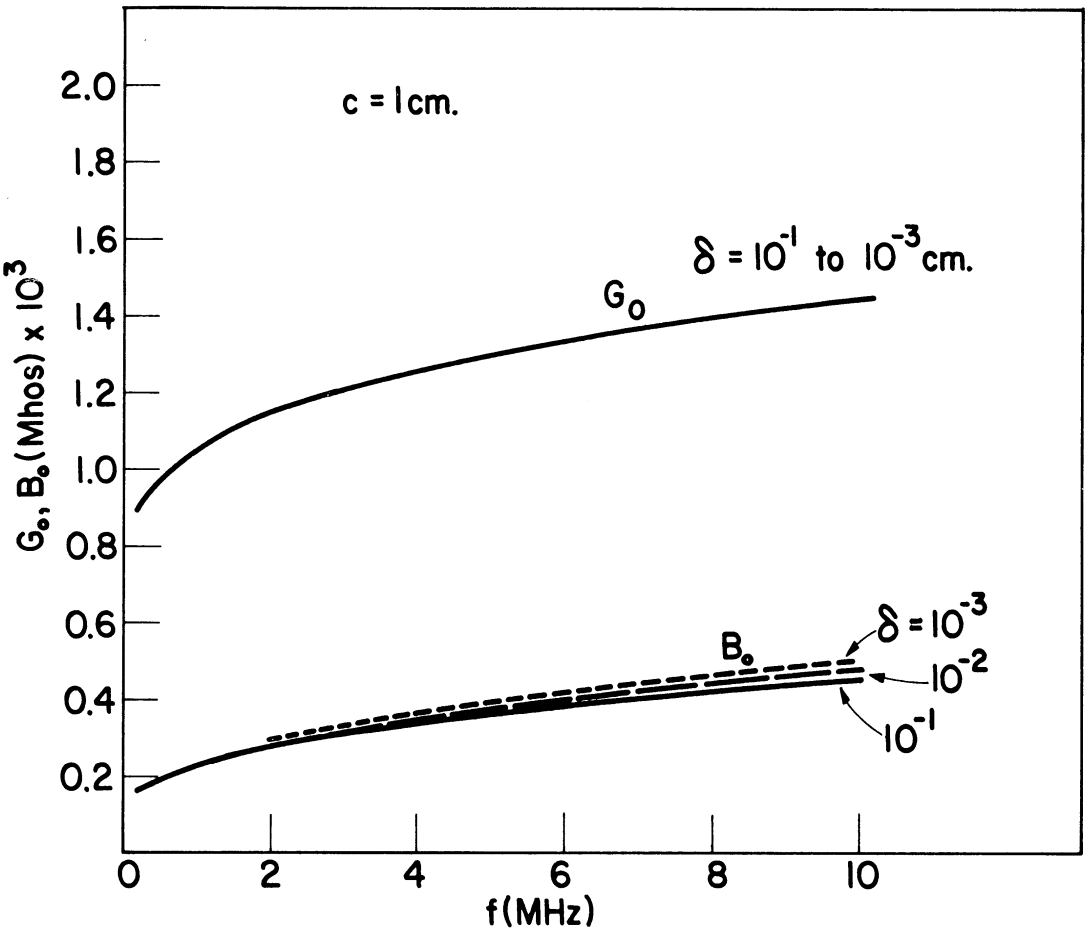

Fig. 2. The free-space infinite cylindrical antenna admittance as a function of frequency with the exciting gap thickness, δ, a parameter, and a radius, c, of 1 cm.

as shown by Miller (1967), the susceptance dependence upon gap thickness increases with increasing frequency. The results of Fig. 2 will be useful to see the perturbing effect of the plasma upon the antenna admittance.

IV. 2 Admittance for the Vacuum Sheath Model

We present in Fig. 3 the antenna admittance as a function of frequency, for an antenna of 1 cm radius, with δ = 1 mm, f_p = 1.5 MHz, ν = 10KHz, T= 1500°K, and a vacuum sheath thickness X, of 5 electron Debye lengths (D_ℓ). The plasma parameters are typical of what one finds in the E to F region of the ionosphere, and the sheath thickness is a reasonable value for an object at floating potential in a plasma. For these parameters, D_ℓ = 1.5998 cm, so that s-c= 7.9988 cm. We note that the antenna diameter is on the same order as D_ℓ , which is a situation where the sheath thickness is dependent on the ratio c/D_ℓ (Laframbois, 1966), and is reduced in value relative to the case where $c >> D_\ell$.

The admittance curve of Fig. 3 exhibits a zero in the susceptance near the plasma frequency, the calculated value changing from inductive to capacitive between 1.5 and 1.5125 MHz. The conductance on the other hand, is seen to reach a definite minimum below the plasma frequency, between 1.475 and 1.5 MHz. Both the conductance and susceptance exhibit maxima below the plasma frequency, at about 0.75 MHz for the conductance, with two maxima for the susceptance at about 0.75 MHz and 1 MHz. The susceptance falls off exponentially with decreasing frequency below the maxima. This resonance below the plasma frequency

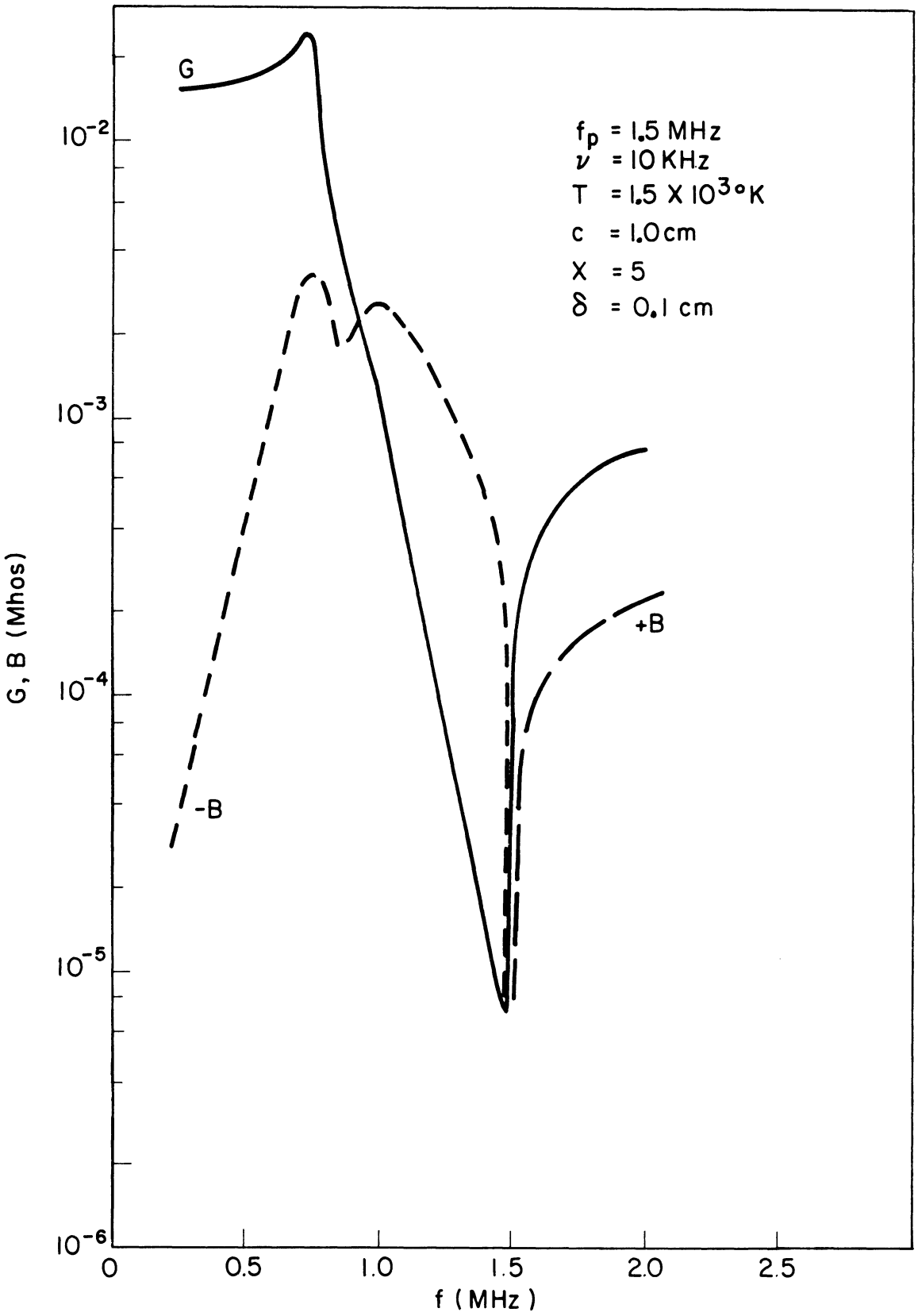

Fig. 3. The infinite antenna admittance as a function of frequency, for the warm plasma, with a vacuum sheath thickness, X, of 5 D_ℓ and a radius of 1 cm.

is quite interesting, and will be discussed further below. If the collision frequency were zero, the conductance from this theory would of course be zero, below the plasma frequency of 1.5 MHz.

For the purposes of comparison, we show in Fig. 4a the admittance of a finite dipole antenna of 1 cm radius and 10 feet (3.048 m) half length (h) immersed in a uniform, cold plasma having the same electron density and collision frequency as for the graph of Fig. 3, calculated from the theory of King et. al (1961). Also shown is the free space antenna admittance. Note that at 1 MHz, $K_{Eo}\, h \approx 6 \times 10^{-2}$, so that the antenna is electrically short. In the discussion to follow it will be assumed that in speaking of finite antennas, we will be dealing only with short antennas, i.e., where $K_{Eo}\, h \leq 0.1$, so that $B_o >> G_o$.

We see that while the susceptance is quantitatively similar to the finite antenna result of Fig. 3 near the plasma frequency, the conductance curves for the two antennas are not even qualitatively similar, varying by several orders of magnitude. It is somewhat surprising to find that the power absorbed by the finite antenna (which is numerically equal to one-half the conductance) exhibits no singular behavior at the plasma frequency, as is shown by the infinite antenna. We may possibly account for this difference in behavior of the finite and infinite antenna near the plasma frequency, in the following way.

We note first of all, that an infinite antenna in free space loses power through the radiation field, (far-field) and surface waves. It is of interest to note that it may be shown from Seshadri's (1965b) results for the far field radiation resistance calculations, and our results of

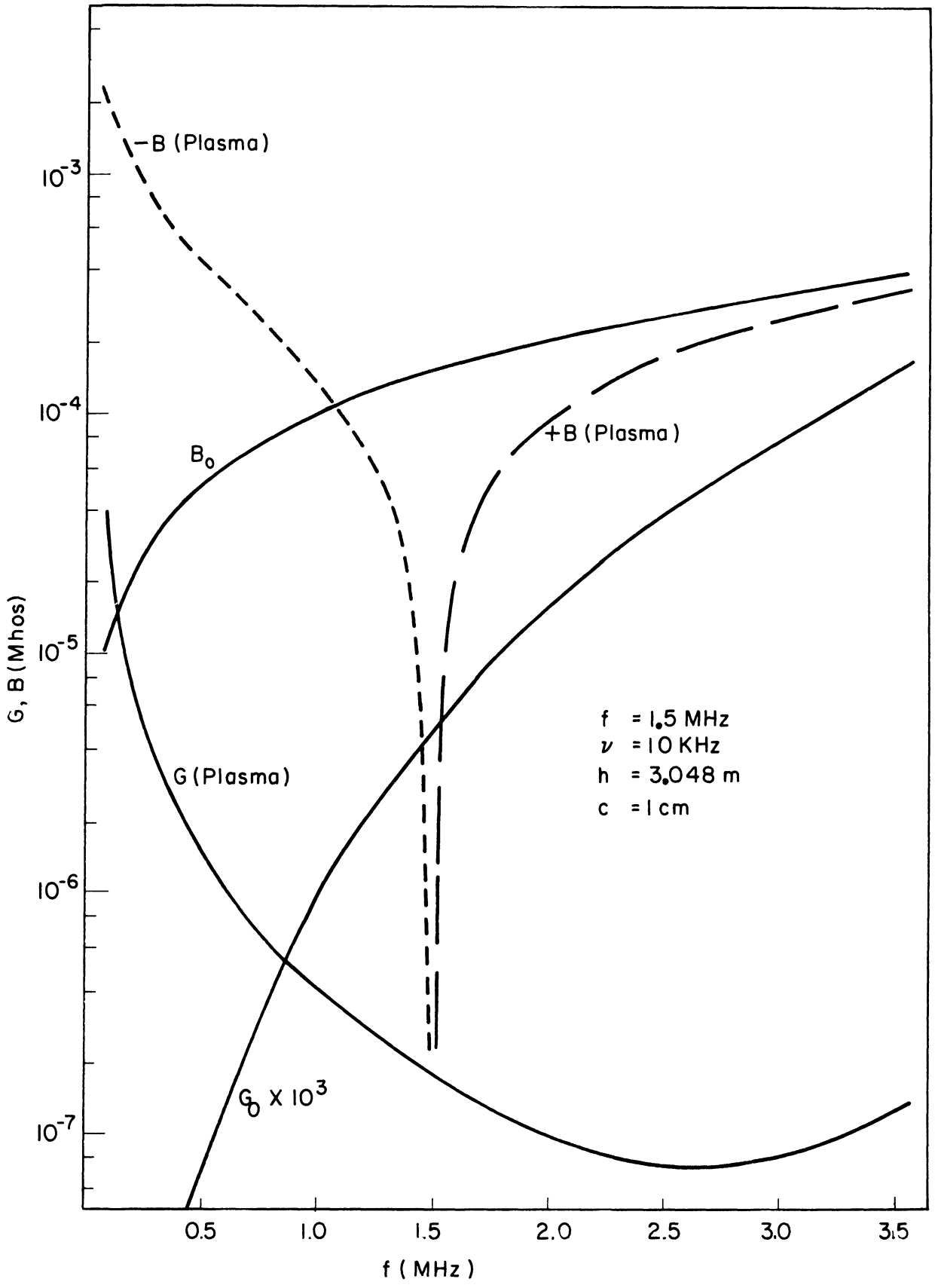

Fig. 4a. The finite antenna admittance (half length h=3.048m) in both free space and the zero temperature plasma.

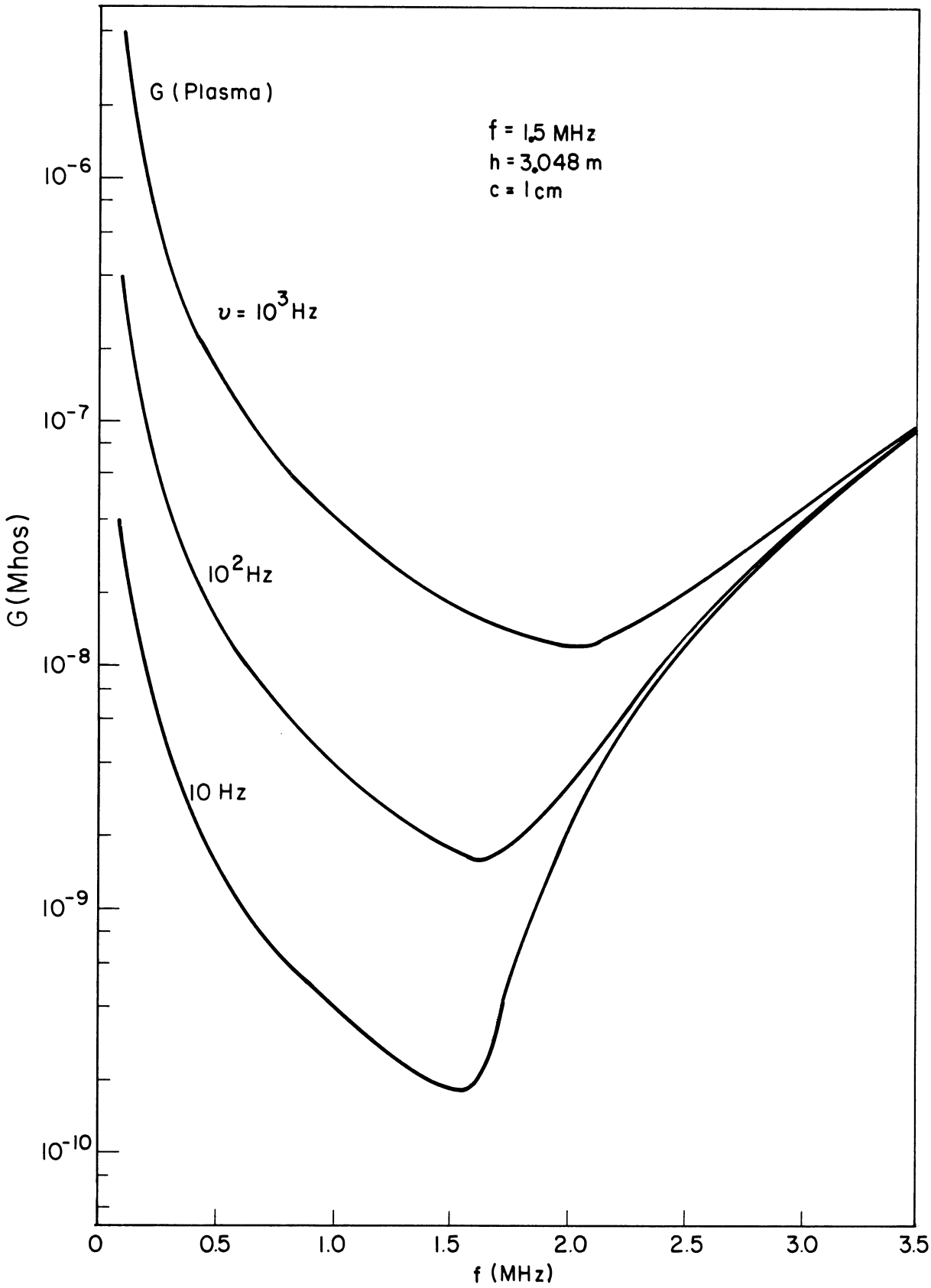

Fig. 4b. The finite antenna conductance in the zero temperature plasma, with the electron collision frequency, ν, a parameter.

Fig. 2, that for the antenna considered here, the surface wave contribution to the antenna conductance exceeds that due to the radiation field, for the free space situation, by a factor of about ten, at 1 MHz. If the antenna is put into a lossy plasma, then collisional absorption, which may be expected to be most important in the near field where the fields are strongest, is an additional way for the antenna to lose power. Now it may be concluded (as will be shown below) that collisional absorption, at least for the magnitude of collision frequency and plasma frequency used here, is small in comparison with the power lost in the radiation field and through surface waves, at 2 MHz. As the operating frequency is decreased towards the plasma frequency, the medium impedance effectively increases, thus decreasing the power carried away by the surface waves and radiation field, with a resulting decrease in antenna conductance, as shown by Fig. 3. The conductance does not decrease to zero of course, because of the near field collisional absorption which becomes then the predominant loss mechanism at and below the plasma frequency.

For the finite antenna in free space on the other hand, power is lost only in the radiation field and the introduction of the lossy plasma medium results in a substantial increase in the antenna conductance, for these same plasma parameters, because of the resulting power loss in the near field due to collisional absorption. The conclusion to be reached from this is that for the short antenna, the near field absorption may be the predominant factor in determining the conductance, near the plasma frequency. This may

be qualitatively shown by writing the free space admittance as

$$Y_o = G_o + iB_o \tag{63}$$

When the antenna is put into a lossy medium of relative permittivity ϵ_r, then

$$Y_o \rightarrow Y \approx \epsilon_r (G_o + iB_o) \approx iB_o \epsilon_r \tag{64a}$$

since $G_o << B_o$. Near the plasma frequency then,

$$G \approx B_o V \tag{64b}$$

and from Fig. 4a, B_o (f=1.5 MHz) = 1.6×10^{-4} MHOS, so that $+ B_o V = 1.7 \times 10^{-7}$ MHOS, while the calculated value for G is 1.8×10^{-7} MHOS. We may also deduce from (64b) that $G \approx \omega^{-2}$ near the plasma frequency, a result which agrees with the calculated values, and which also shows that the conductance does not have a minimum near f_p, depending upon ν and ω alone.

As a further illustration of the near field influence on the finite antenna conductance in the lossy plasma, we show the conductance only in Fig. 4b for collision frequency values of 10, 10^2 and 10^3 Hz. The susceptance was negligibly different from that shown for $\nu = 10^4$ Hz in Fig. 4a, and so is not included. We see that as ν is decreased in value, the conductance decreases proportionately except near f_p where a minimum begins to appear at 10^2 Hz and which is quite pronounced at 10 Hz. This minimum occurs now since

for ν = 10 Hz, $B_o V \approx G_o$, and the resulting minimizing effect of $G_o \epsilon_r$ is large enough to show up. Thus a minimum exists in the finite antenna conductance, similar to that of the infinite antenna, but requiring a very much lower electron collision frequency than is required in the case of the infinite antenna. We may briefly note that physically, the finite antenna behavior results from the reactive near field interacting with the imaginary part of the plasma permittivity (which is determined by electron collisions) to produce in-phase currents larger than those produced by the in-phase field, unless, as noted, the collision frequency is very low.

We must remember in comparing these results that the finite antenna theory is for the cold palsma while the infinite antenna results are for the compressible plasma, and as such may not be meaningfully related. Results will be given subsequently for the infinite antenna in the cold plasma, so that the effect of the temperature may be shown, and in that case a comparison of the two antennas may be more significant. It is in addition of interest to compare the finite antenna results with some actual antenna measurements in the ionosphere given by Heikkila (1965a) which are given in Fig. 5. This data was obtained using a hemispherical antenna 11.6 cm in diameter. A rather sharp maxima may be seen in the admittance, below the plasma frequency, a feature not exhibited by the calculated results of Fig. 4. It should be observed that the magnetic field may have an influence on the measured admittance values of Fig. 5, but is not included in the theoretical calculations.

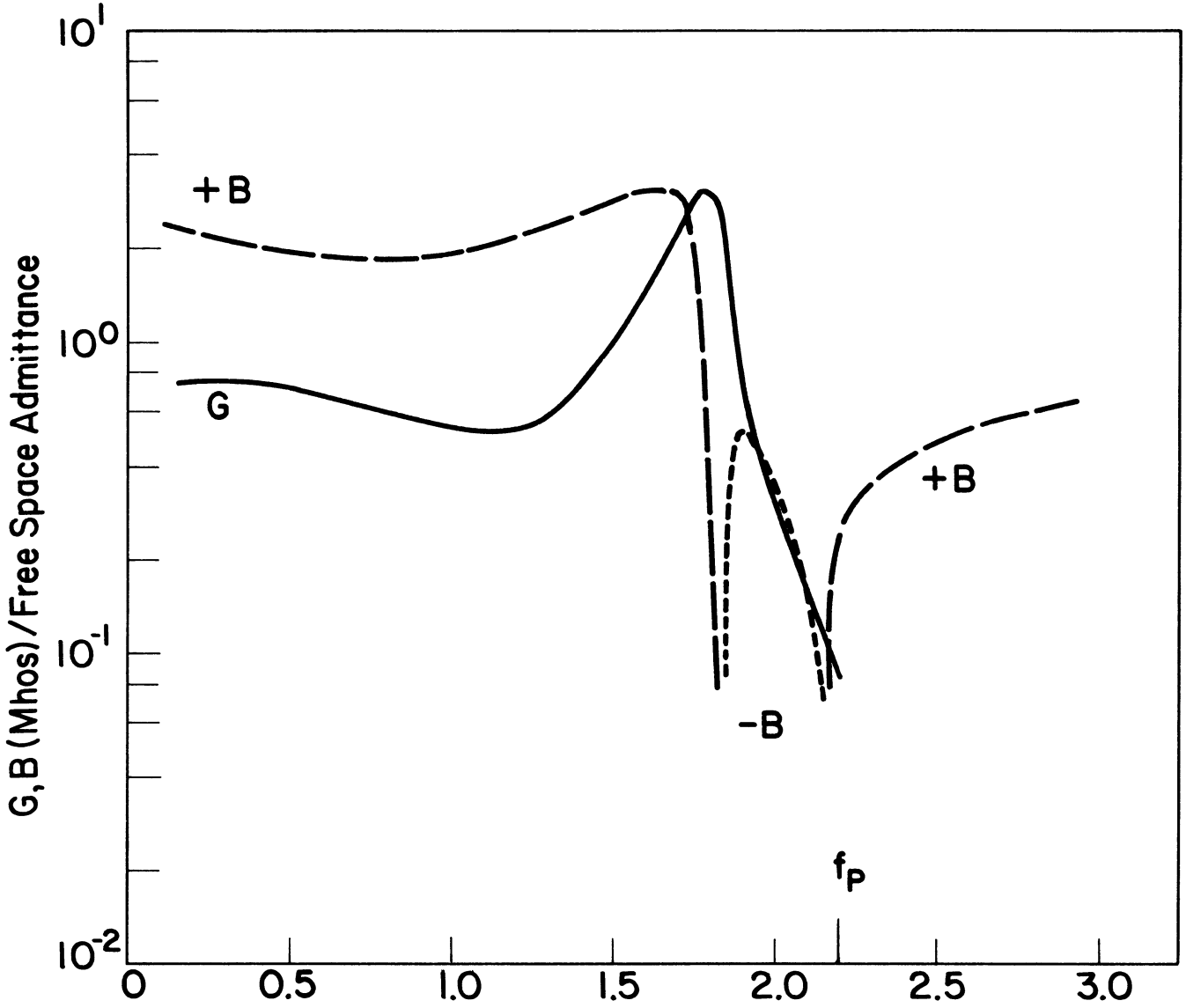

Fig. 5. Experimentally measured antenna admittance in the ionosphere, due to Heikkila (1965a).

The discussion presented above may be briefly summarized by noting that generally, the conductance of the infinite antenna is decreased and that of the short finite antenna is increased with respect to free space values, when the antenna is in a lossy plasma and operated near the plasma frequency. In addition, it appears that the conductance of both near the plasma frequency is primarily a function of the near field. The susceptance of both is found to change from capacitive to inductive at the plasma frequency.

In order to get some idea of the influence of the finite electron temperature on the infinite antenna admittance, Fig. 6 shows the admittance for the same parameters as Fig. 2, except that T is now zero. In spite of the fact that $D_\ell \longrightarrow 0$ when $T \longrightarrow 0$, the same numerical value of vacuum sheath thickness is used in obtaining the results of Fig. 6 so that we may to some extent attempt to separate the sheath and temperature effects. It may be seen that the susceptance for the zero temperature case is similar to that for the finite temperature curve of Fig. 2, the primary difference being that the zero temperature susceptance is slightly more capacitive, except in the vicinity of 0.85 MHz, where the zero temperature susceptance does not exhibit the oscillation present in the former case. The conductance is also practically unchanged above the plasma frequency, but is considerably different for $f < f_p$, where the zero temperature conductance is everywhere less than that when $T = 1.5 \times 10^3$ ^oK. A sharp minimum in the conductance is again found at about 1.475 MHz, but with about one-fifth the magnitude of the finite temperature case, about the same ratio shown by the conductance maximum near

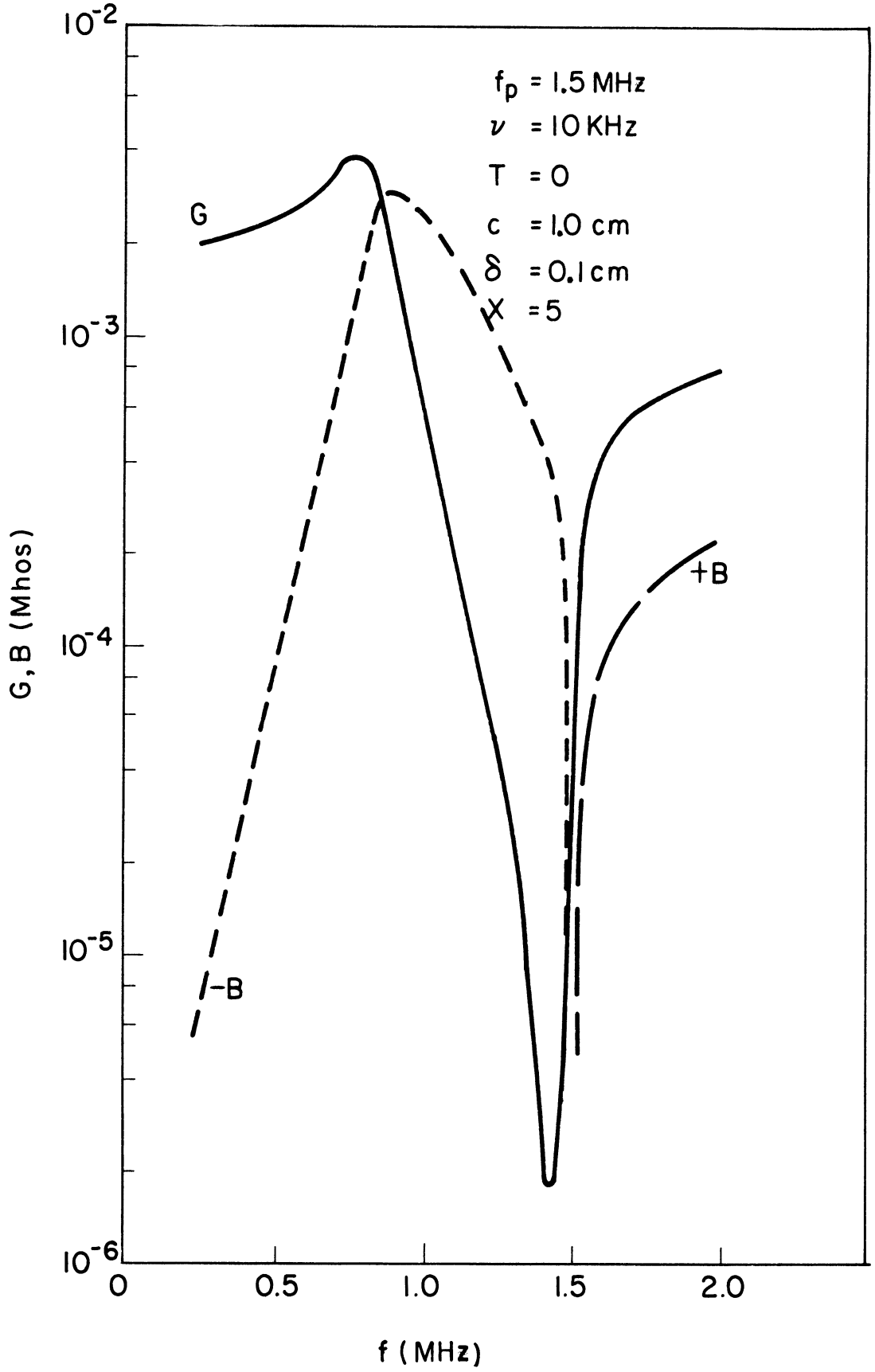

Fig. 6. The infinite antenna admittance as a function of frequency with a vacuum sheath thickness of 5 D_ℓ, for the zero temperature plasma.

0.7 Mhz. The significance of the change in conductance with temperature will be considered further below.

The antenna admittance for zero sheath thickness and with the same parameter values as Figs. 2 and 6 are shown respectively on Figs. 7 and 8, for $T=1.5\times10^{3}\ ^{o}K$ and $T=0\ ^{o}K$. There is now a noticable difference in both the conductance and susceptance for all the frequency range shown for the two values of temperature. The zero temperature susceptance is again more capacitive than the finite temperature case, for frequencies above 0.7 MHz, but does not peak below f_p, so that below 0.7 MHz, the zero temperature susceptance is now more inductive than the latter case. The conductance is again less for the zero temperature case, and like the susceptance does not peak below f_p as does the finite temperature result. A conductance minimum is again seen below f_p, but is broader in each case than that observed for the $5D_\ell$ thick sheath. Above f_p, the finite temperature conductance for the sheathless case differs by less than 1 percent from the $5\ D_\ell$ thick sheath values for both temperatures.

Perhaps the most interesting and significant feature of the results shown in Fig. 3, 6, 7, and 8 is the admittance maxima exhibited by all but the sheathless, zero temperature case. This is especially so because the experimental results of Heikkila in Fig. 5 also show an admittance maxima below the plasma frequency. The calculated results for the short linear antenna in a cold plasma of Fig. 4 have no comparable maxima, on the other hand, but do bear a remarkable similarity to the corresponding infinite antenna curves of Fig. 8. This similarity would seem to strengthen a supposition previously stated, that the near fields of both the infinite and

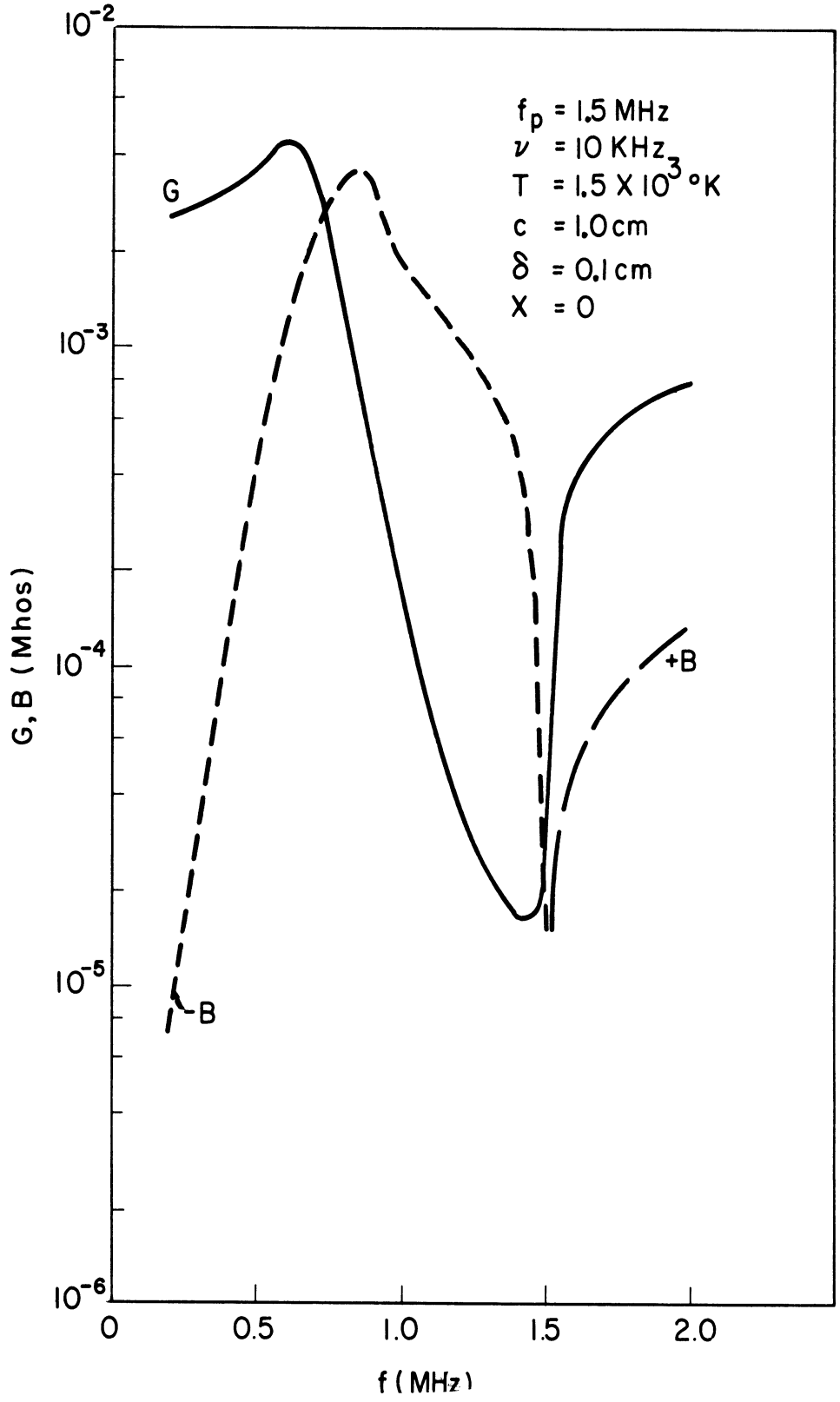

Fig. 7. The infinite antenna admittance as a function of frequency for the warm plasma, with zero sheath thickness.

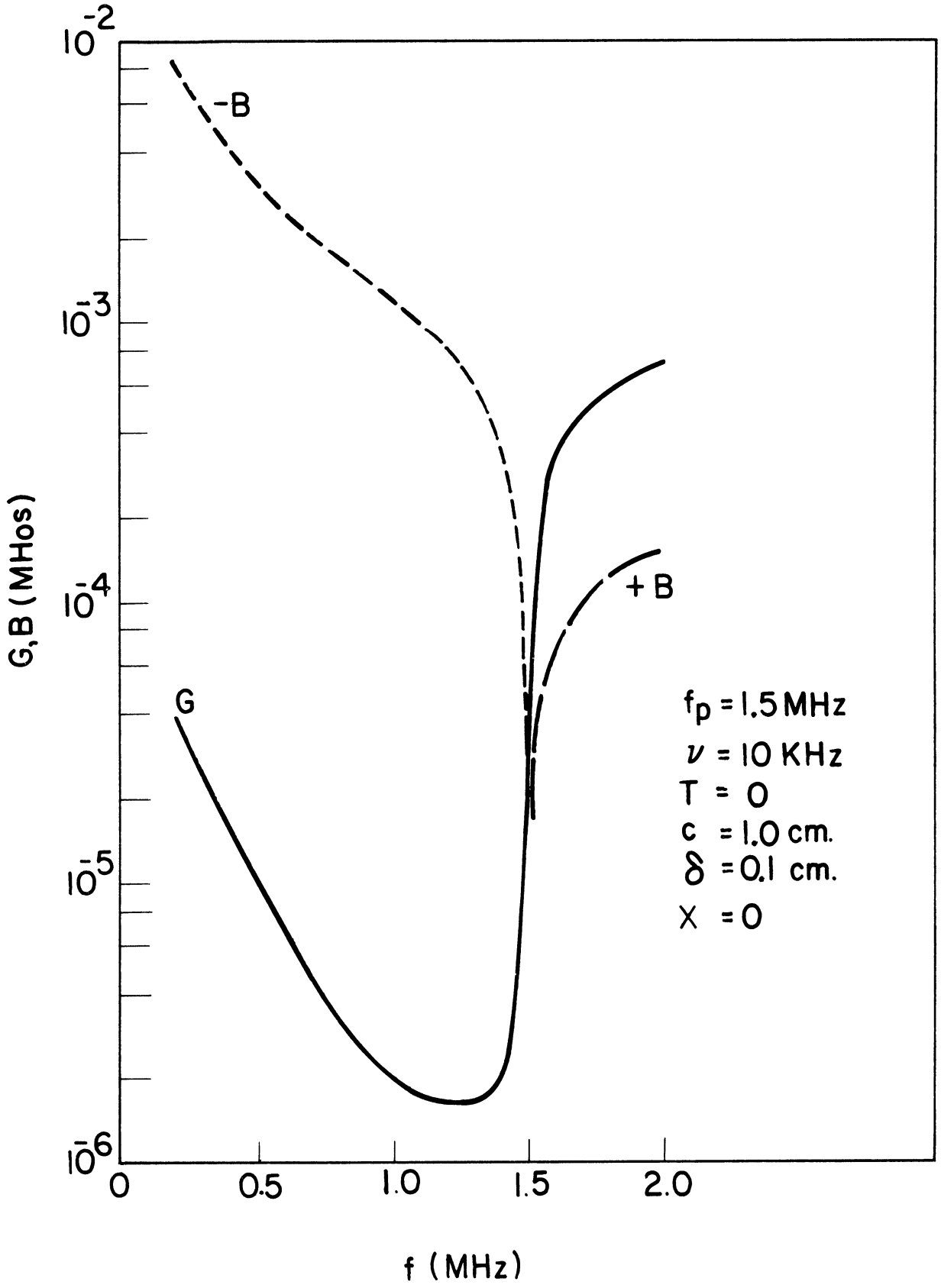

Fig. 8. The infinite antenna admittance as a function of frequency for the zero temperature plasma and zero sheath thickness.

finite antennas exercise the predominant influence on the admittance near, and below, the plasma frequency, so that consequently, it may be resonable to infer the qualitative frequency variation of the finite antenna in this frequency range from the infinite antenna results.

A tentative conclusion might be reached from these results that a finite plasma electron temperature and/or a sheath are required to obtain an admittance maxima below the plasma frequency. This admittance maxima appears to be related to the rectification resonance described by Takiyama (1960) and at first thought to occur at the plasma frequency. Subsequent consideration by Harp and Crawford (1964), has indicated that the resonance lies below f_p and is related to the sheath thickness and electron temperature, a result which our findings would seem to support.

It is thus found from these calculations, that the susceptance of the infinite antenna shifts in the capacitive direction with a decrease in electron temperature, on both sides of the plasma frequency. Removing the sheath decreases the magnitude of the susceptance, in both the capacitive and inductive susceptance regions. The conductance is primarily affected by the sheath and finite temperature below the plasma frequency, where a decrease in temperature or sheath thickness produces a decreased conductance. It appears that the EK wave is only weakly excited above the plasma frequency, but plays a greater role in the antenna behavior below the plasma frequency.

This finding that the EK wave has only a weak effect upon the antenna conductance above f_p is in contrast to the results of Wait (1966),

Seshadri (1965b) and Cohen (1962), who found the EK wave to be quite strongly excited in their analyses. Wait and Cohen treated finite antennas however, and their results may possibly be attributed to the small antenna dimensions. Seshadri did analyze the infinite cylindrical antenna, but considered only the radiation fields, and found that the power in the EK and EM modes were on the same order of magnitude. Since the present treatment includes the effect of the surface waves and near field absorption, it might be concluded that the power put into surface waves and the near field is less sensitive to electron temperature than is the radiation field. In addition, since as has been previously mentioned, the radiated power is less than that lost by these latter means, the effect of the electron temperature on the radiated power is masked.

Because the electron temperature does affect the antenna susceptance below the plasma frequency, Fig. 9a shows the admittance at a single frequency, 1.4 MHz, as a function of the temperature, with the electron collision frequency a parameter. Fig. 9b presents the results plotted as a function of the electron collision frequency, with the temperature now a parameter. The T = 0 curve of Fig. 9b shows the conductance increasing in direct proportion to the collision frequency, a result also obtained from the finite antenna analysis. It is also of interest to see that the susceptance has relatively little or no dependence upon the collision frequency, a result which again is obtained for the finite antenna. The most interesting aspect of 9a is that as the electron temperature increases, the conductance becomes less sensitive to changing collision frequency, an effect which is shown in 9a as a coalescing of

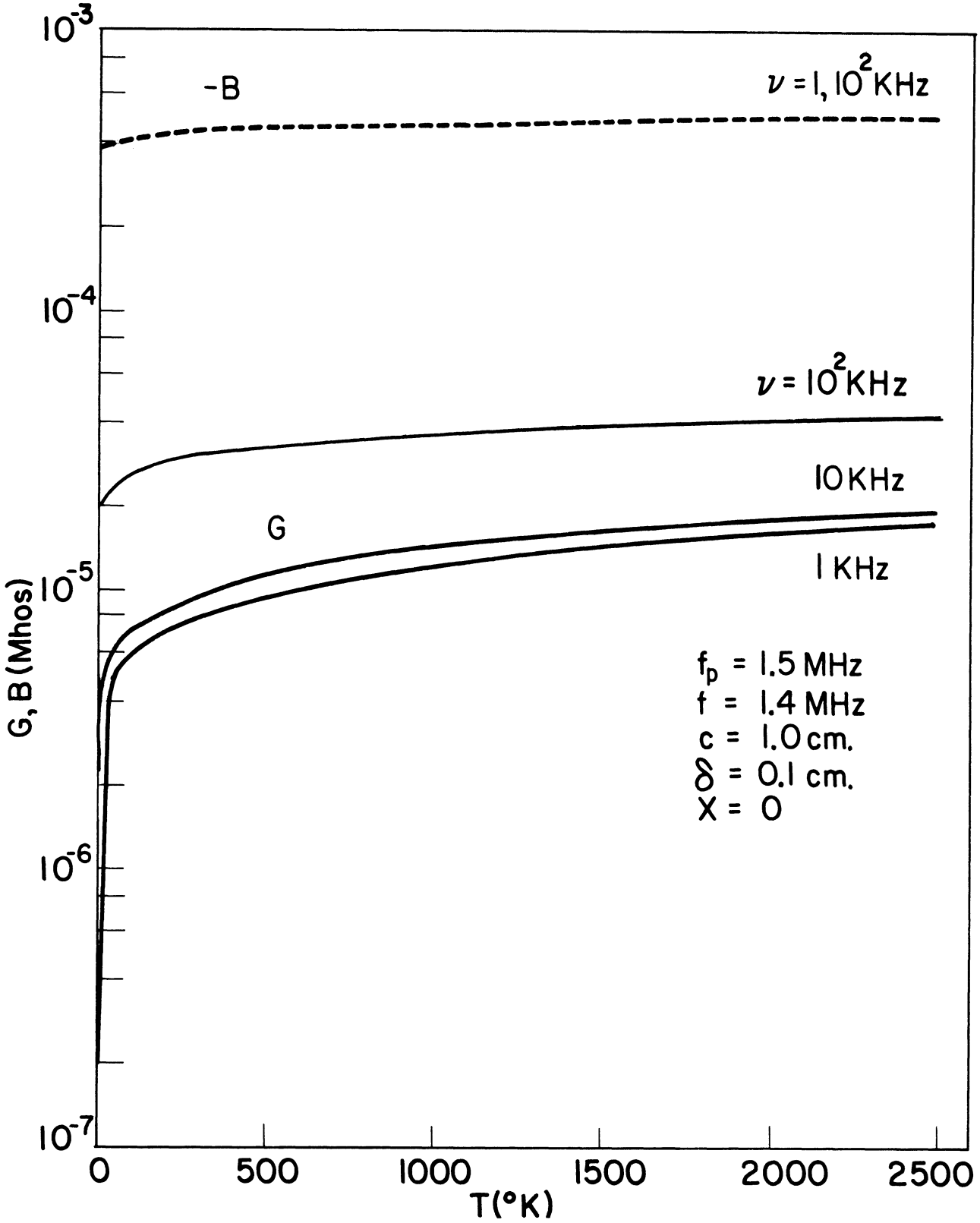

Fig. 9a. The infinite antenna admittance as a function of electron temperature at a frequency of 1.4 MHz (f_p = 1.5 MHz), with the electron collision frequency a parameter.

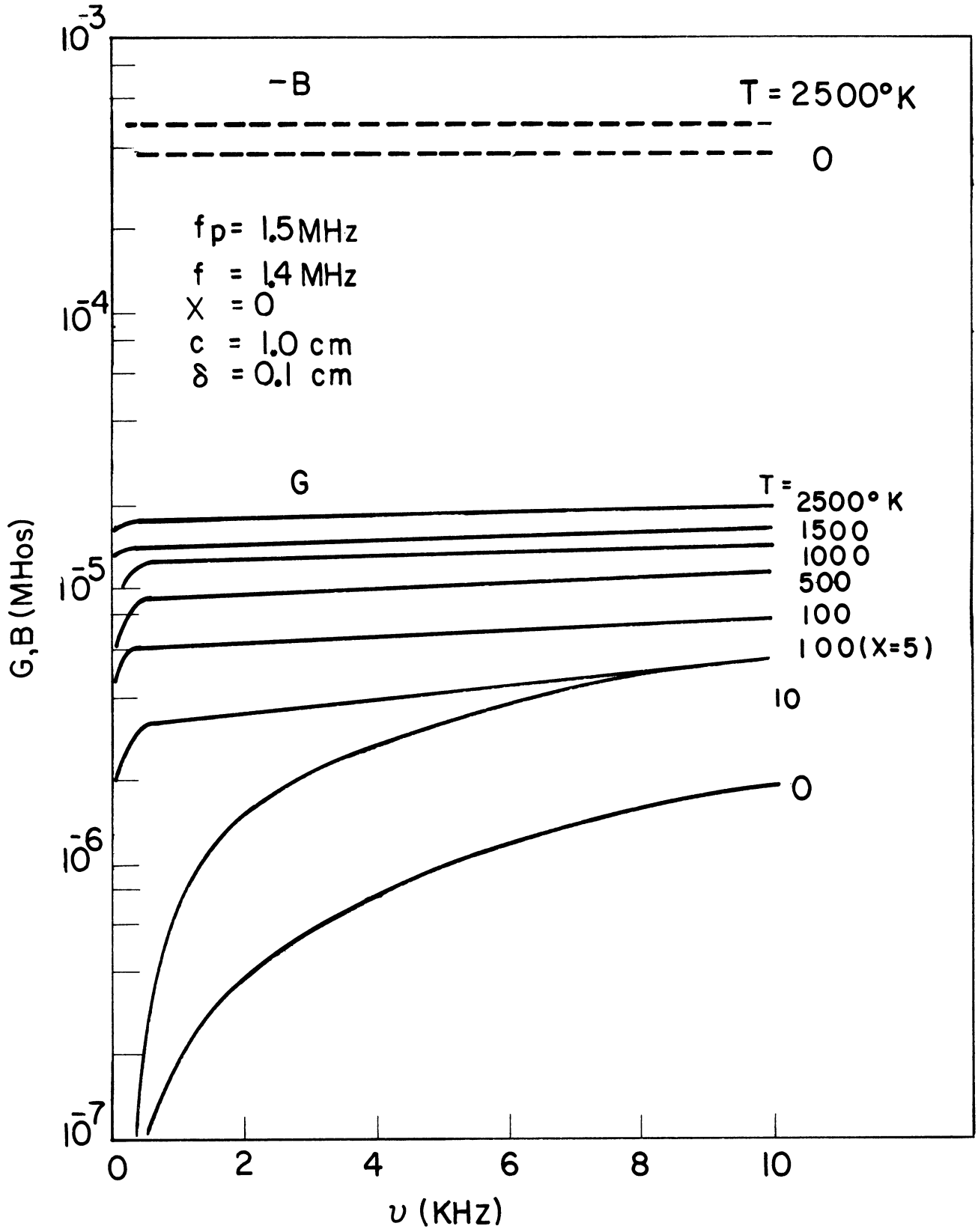

Fig. 9b. The infinite antenna admittance as a function of electron collision frequency at a frequency of 1.4 MHz (f_p = 1.5 MHz), with the electron temperature a parameter.

the various collision frequency curves with increasing temperature. Thus is is seen that we may possibly interpret a large conductance below the plasma frequency, if we use the cold plasma theory, to indicate a larger collision frequency than is actually the case.

It is of interest to note that the same range of variation in the electron collision frequency at a frequency of 2 MHz and electron temperatures of O ^{o}K and 1, 500 ^{o}K produced less than a 1 percent change in both the conductance and susceptance. This result for the conductance indicates that collisional absorption is relatively unimportant at this frequency in determining the power lost by the antenna, compared with the radiated field and surface wave. The collisional effects increase in importance as the plasma frequency is approached.

Figure 10 presents the antenna admittance variation, at 1.0 MHz, as a function of the vacuum sheath thickness, with the electron temperature a parameter, and a constant electron collision frequency of 10 KHz. We see that an increasing sheath thickness leads to increasing conductance and increasing inductive susceptance, over the range of sheath thickness shown.

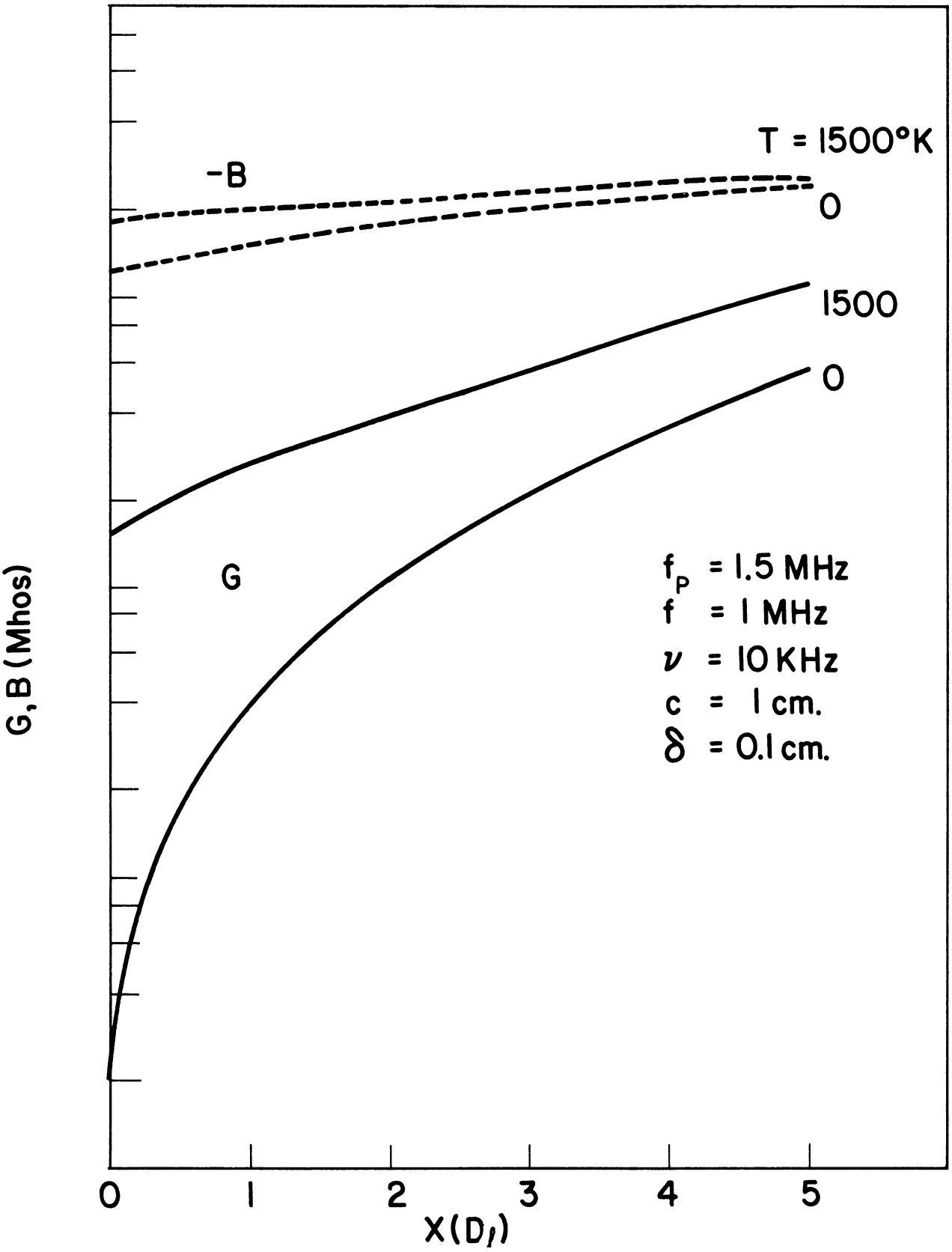

Fig. 10. The infinite antenna admittance as a function of vacuum sheath thickness at a frequency of 1.0 MHz (f_p = 1.5 MHz), with the electron temperature a parameter.

IV. 3 Summary

As was stated in the introduction to this report, we would ideally like to analyze the impedance characteristics of a finite dipole antenna immersed in a plasma such as the ionosphere, taking into account compressibility and sheath effects, as well as the ionospheric magnetic field. We would in addition like to do a time domain analysis of such an antenna in order to explicitly demonstrate the relaxation resonance effect. Because of the extreme complexity of even the first part of this problem, we have chosen to investigate instead, the plasma-immersed, infinite, cylindrical dipole antenna, and have for the present, neglected the static magnetic field.

The reasons for this approach have been the fact that the infinite dipole antenna could be treated exactly, even to including the inhomogeneous sheath and magnetic field, and the anticipation that the finite antenna results could at least be qualitatively inferred from the infinite antenna results. The results presented here for the zero temperature plasma, for both the finite dipole and the sheathless infinite antenna, are in qualitiative agreement below the plasma frequency, and indicate the reasonableness of inferring the finite antenna behavior from the infinite antenna results, if care is used.

We have found that for the infinite antenna, the admittance is relatively unaffected by the plasma compressibility and sheath above the plasma frequency. A decrease in temperature results in a decreased conductance and a more capacitive susceptance, while a decrease in the vacuum sheath thickness causes a somewhat smaller conductance and

a less capacitive susceptance. Below the plasma frequency however, these effects become important in determining the antenna susceptance, where a decrease in the temperature leads to smaller conductance and less inductive susceptance, while a decrease in sheath thickness leads to a smaller conductance and generally more inductive susceptance. In particular, an admittance maximum is found below the plasma frequency when there is a sheath or finite electron temperature, but which is absent for the zero temperature, sheathless situation. This admittance maximum appears to be related to the rectification resonance of Takiyama.

The influence of the plasma temperature and sheath on the location of the admittance maximum have not been established here; because of the lengthy nature of the calculations, it has not been possible to do an extensive parametric study of the admittance. However, we have found from the numerical results presented, that for a fixed sheath thickness of 5 D_ℓ, decreasing the temperature from 1,500 ^{o}K to 0 ^{o}K results in practically no shift in the location of the maximum, though the magnitude is reduced by a factor of about 5. Similarly, decreasing the sheath thickness from 5 to 0 D_ℓ at a fixed temperature of 1,500 ^{o}K produces a slight downward shift in the location of the conductance maximum from about 0.75 MHz to 0.6 MHz, although the susceptance maximum remains at about the same frequency, 0.8 MHz. This may be a question worth pursuing further, since some other theoretical results, based on a very much simpler approach by Harp and Crawford, (1964) indicate that the rectification resonance should shift upwards towards the plasma frequency with decreasing sheath thickness. It may be that the surface

waves which can propagate on the infinite antenna, even below the plasma frequency when there is a sheath, can significantly alter our results in this regard, compared with the finite antenna.

It has also been found for the infinite antenna that temperature and collisional effects are to an extent, equivalent below the plasma frequency, each acting to increase the antenna conductance. Above the plasma frequency, neither the temperature nor collision frequency exercise much influence over the admittance. The latter occurs because the free space conductance and susceptance are of nearly equal magnitude, and therefore not sensitive to the small imaginary part of ϵ_r determined by the collision frequency.

A change in the sign of the susceptance of the infinite antenna is observed above, but within 1% of the plasma frequency, as nearly as can be found from the calculations. While the sheath may be expected to influence the location of the susceptance zero, the sheath thickness for a realistic electron temperature is so small compared with the EM wavelength that this is not a determining factor here. A conductance minimum is also found near to, but below the plasma frequency. This minimum is broader for the sheathless case and farther from the plasma frequency than is the corresponding 5 D_ℓ thick sheath result. This conductance minimum may be explained on the basis of a cut off in the propagation of the surface and space waves as the plasma frequency is approached.

We have further found that, while the finite antenna in a cold, lossy plasma does exhibit a change in sign of the susceptance in the vicinity of the plasma frequency, the conductance has no minimum such

as is found for the infinite antenna, unless the collision frequency to excitation frequency ratio is on the order of, or lower than, the finite antenna free space conductance to susceptance ratio. This behavior of the short finite antenna has been explained here by observing that in a lossy plasma, the reactive antenna near field interacts with the imaginary part of the plasma permittivity to produce in-phase currents larger than those produced by the much smaller in-phase field. If the plasma is in addition, compressible, it appears that the conductance may be made larger, but we cannot conclude from our study whether or not the conductance of the finite antenna would then show a minimum near the plasma frequency, as is found for the infinite antenna. This would appear to depend upon the antenna length, which even when short compared with the EM wavelength, may be long compared with the EK wavelength. It is interesting to mention that the admittance of a spherical dipole in the ionosphere, given by Heikkila (1965a), has no conductance minimum at the plasma frequency, but does exhibit an admittance maximum below the plasma frequency.

V. Comments and Conclusions

An analysis of the admittance of an infinite cylindrical antenna excited by a circumferential voltage gap, and immersed in a compressible, lossy plasma medium has been discussed. The sheath which forms about a body at floating potential in a plasma has been represented by a vacuum sheath model, where the actual sheath is replaced by a free space layer, and an inhomogeneous sheath model, where the actual sheath inhomogeneity is taken into account. Numerical results for the admittance over a frequency range including the electron plasma frequency, and for other parameter values typical of the ionosphere have been given for the vacuum sheath model. The motivation for this work has been a desire to investigate the influence of a plasma upon the impedance characteristics of an antenna immersed in it, to possibly acquire a better qualitive understanding of the radio frequency probe as a tool for plasma, and thus ionospheric, diagnostics.

The numerical results which have been obtained are significant in a number of respects. It has been shown that even the relatively low electron collision frequencies typical of the lower ionosphere (E and F regions) are large enough to significantly increase the conductance of a short (compared to the EM wavelength) antenna immersed in the ionospheric type plasma of zero temperature. We have also found from the infinite antenna analysis that the finite temperature and collisional effects are interdependent, thus further increasing the importance of taking the collisions into account, especially of course, below the plasma frequency. A further finding of interest is the presence of an admittance maximum for the infinite antenna below the plasma frequency, which disappears only when there is no sheath and the electron

temperature is zero. Although such a feature has been found by others for the quasi-static approximation, this is the first time that we are aware of a solution to the full boundary value problem for the compressible plasma which shows this property.

A comparison of the finite antenna admittance in a zero temperature plasma, using King's theory, with the only infinite antenna results where a direct comparison can be made, the zero temperature, sheathless case, shows there to be a good qualitative similarity in their behavior below the plasma frequency. This similarity is significant in that, while it does not guarantee we are on the right track in hoping to learn something about the finite antenna's behavior from results for the infinite antenna, it at least does not contradict the possibility of doing this.

A number of objections, other than that to the infinite antenna analysis used here, may be raised to the numerical results we have obtained. When we consider that the medium in which we are interested is the ionosphere, the inclusion of a static magnetic field in the analysis is obviously desirable. In addition, the more accurate representation of the sheath by the inhomogeneous sheath model, rather than the vacuum sheath model employed exclusively here to obtain the numerical results presented, would be also desirable. Some preliminary numerical computations have been made for both the inhomogeneous sheath model, but without a static magnetic field, and the vacuum sheath, zero temperature case, with a z-directed magnetic field. These computations are considerably more lengthy, especially the former, than those required to obtain the results given here. However, it is anticipated that some admittance curves as a

function of frequency will be obtained for these situations, and these results will be reported on subsequently. It appears that it may also be feasible to investigate the warm plasma with the static magnetic field and possibly also including the inhomogeneous sheath. A decision on whether to extend our analysis to this situation will be made after some of the cold plasma, static magnetic field results have been obtained.

We should also mention that the representation of the plasma by the fluid equations rather than using the more rigorous kinetic approach is open to objection, particularly since the possibility of Landau damping is not encompassed in the fluid approach. In the absence of collisions, the fluid approach predicts zero conductance below the plasma frequency, whereas the kinetic theory shows there to be some lossyness due to Landau damping. The fluid equations represent an averaging of the plasma response, which while seemingly reasonable in regions where the change in plasma properties occur slowly in comparison with the Debye length, may be on less safe ground in regions of rapid change, such as the sheath. A study by Pavkovich (1963) for the planar geometry contains a comparison between fluid and kinetic results for the impedance of an inhomogeneous sheath, which is claimed to show the unrealiability of the fluid approach. However, it appears that the author's conclusion about this may be somewhat prejudiced a priori in favor of the kinetic theory, as the results obtained by the two approaches do not seem that much at variance.

It has been noted that neglect of electron collisions does not appear to be a reasonable assumption for the warm plasma. Even in the case of a cold plasma, the collisions may have a strong influence on the admittance

of a short antenna. Thus it would seem that radiation resistance calculations which are carried out using the far fields, are not particularly useful, since they of necessity are for the lossless medium. A further objection can be raised to an analysis such as that of Kuehl (1966), which while using the kinetic approach for finding the radiation resistance of a short antenna, (collisions are neglected here also) assumes a specified current distribution, and is actually a solution for a current source rather than a physical antenna. In addition, in order for the antenna to be short compared with the EK wavelength, (an implicit assumption in the analysis) an antenna length on the order of a few centimeters or less would be required for the ionospheric plasma. This is a clearly impractical length for actual experimentation at the frequencies involved, since the reactive impedance component would be very much larger than the resistive component of interest. It is interesting however to note that Kuehl (1967), presents some numerical results for the model mentioned above, comparing the resistance of the antenna obtained from both the hydrodynamic and kinetic theories, for the collisionless plasma. His findings show that for antennas more than a few D_ℓ long, the two theories produce nearly identical resistance values, above the plasma frequency. This indicates that the hydrodynamic approach is not an unreasonable one to use, particularly if electron collisions are also included in the analysis, so that the hydrodynamic neglect of Landau damping may become less important.

Appendix A: Singularities of the Current Integral

The purpose of this discussion is to show that while the separate parts of the integrand of Eq. (35) have non-integrable singularities at $\beta=K_{Eo}$, their sum does not. If we examine the free space current first, given by Eq. (36), we find that

$$I_{or}(z,\omega) = + \frac{4 V_o K_{Eo}}{\eta_o \pi} \int_0^{K_{Eo}} \frac{\cos(\beta z)\, \bar{S}(\beta)}{\lambda_{Eo}^2 (J_c^2 + Y_c^2)}\, d\beta \qquad \text{(A1a)}$$

$$I_{oi}(z,\omega) = + \frac{2 V_o c K_{Eo}}{\eta_o} \int_0^{\infty} \frac{\cos(\beta z)}{\lambda_{Eo}} \bar{S}(\beta) \left[\frac{J_c' J_c + Y_c' Y_c}{J_c^2 + Y_c^2} \right] d\beta \qquad \text{(A1b)}$$

where J_c and Y_c are the Bessel and Neumann functions of order zero and argument $\lambda_{Eo}c$ and the prime denotes differentiation with respect to argument. Now the singular part of I_{or} is contributed only by the denominator, so we examine its behavior as $\beta \to K_{Eo}$. Using the small argument forms for J and Y, we obtain

$$\frac{1}{\lambda_{Eo}^2 (J_c^2 + Y_c^2)} \approx \frac{1}{\lambda_{Eo}^2 Y_c^2} \approx \frac{1}{\left[2 \lambda_{Eo} \ln(\lambda_{Eo} c)\right]^2} \qquad \text{(A2)}$$

If we let

$$\beta = K_{Eo}(1-\Delta) \quad ; \quad \Delta \ll 1$$

then

$$\lambda_{Eo}^2 \approx 2 K_{Eo}^2$$

and the singular part of the integrand of (A1a) is given by

$$\frac{\pi^2 d\Delta}{8 K_{Eo}^2 \Delta \left[\ln(\sqrt{2\Delta}\, K_{Eo} c)\right]^2} \qquad \text{(A3)}$$

$$= \frac{\pi^2 d\Delta'}{4 K_{Eo}^2 \Delta' (\ln \Delta')^2}$$

which is integrable at $\Delta' = 0$ since

$$\int \frac{dx}{x(\ln x)^2} = \frac{1}{\ln(x)}$$

However, when we consider the singular part of the integrand of $I_{oi,}$ we have

$$\frac{J_c' J_c + Y_c' Y_c}{\lambda_{Eo}(J_c^2 + Y_c^2)} \approx \frac{Y_c'}{\lambda_{Eo} Y_c}$$

$$\approx \frac{2}{\pi \lambda_{Eo}^2 c\, Y_c}$$

$$\approx \frac{1}{\lambda_{Eo}^2 c \ln(\lambda_{Eo} c)} \qquad \text{(A4)}$$

Using the same scheme as for $I_{or,}$ we find, using (A4), that the singular part of the I_{oi} integrand becomes

$$\frac{d\Delta'}{K_{Eo}^2 c\, \Delta' (\ln \Delta')} \qquad \text{(A5)}$$

which is not integrable at $\Delta' = 0$ since

$$\int \frac{dx}{x \ln x} = \ln(\ln x)$$

The plasma contribution to (35) can be investigated in a similar fashion. We require for this purpose, the Wronshian expression for the small argument limits, which are

$$W(c, s) \approx 4i \ln (c/s) / \pi$$

$$W(c', s) \approx 4i / \pi \lambda_{Eo} c$$

$$W(c, s') \approx -4i / \pi \lambda_{Eo} s$$

$$W(c', s') \approx 2i (c/s - s/c) / \pi$$

We may show that near $\beta = K_{Eo}$,

$$\bar{A}_m^R \approx \frac{K_{Eo} \bar{S}(\beta) H_o^{(2)'}(\lambda_{Eo} s)}{\lambda_{Eo}^2 W(c, s')} \tag{A6}$$

Thus the real and imaginary parts of ΔI, denoted by ΔI_r and ΔI_i, become, in the vicinity of $\beta = K_{Eo}$

$$\Delta I_r = \frac{-4 V_o K_{Eo}}{\eta_o \pi} \int \frac{\cos(\beta z) \bar{S}(\beta)}{\lambda_{Eo}^2 (J_c^2 + Y_c^2)} d\beta$$

$$\approx \frac{-4 V_o K_{Eo}}{\eta_o \pi} \int \frac{\cos(\beta z) \bar{S}(\beta)}{\lambda_{Eo}^2 Y_c^2} d\beta \tag{A7}$$

$$\Delta I_i = -\frac{8 V_o K_{Eo}}{\eta_o \pi} \int \frac{\cos(\beta z) \bar{S}(\beta)}{\lambda_{Eo}^2 |W(c, s')|} \left[\frac{J_s' J_c + Y_s' Y_c}{J_c^2 + Y_c^2} \right] d\beta$$

$$\approx \frac{-8 V_o K_{Eo}}{\eta_o \pi} \int \frac{\cos(\beta z) \bar{S}(\beta)}{\lambda_{Eo}^2 |W(c, s')|} \frac{Y_s'}{Y_c} d\beta$$

$$\approx \frac{-4 V_o K_{Eo}}{\eta_o \pi} \int \frac{\cos(\beta z) \bar{S}(\beta)}{\lambda_{Eo}^2 Y_c} d\beta \tag{A8}$$

where J_s and Y_s are zero order Bessel and Newmann function of argument $\lambda_{Eo}s$. We see upon comparing (A7) and (A8) with (A1) to (A4) that the ΔI and I_o integrals, in the vicinity of $\beta=K_{Eo,}$ are equal but of opposite sign, thereby cancelling the non-integrable singualrities. Note that while singular parts of (35) thus cancel, the integrand does not become zero. That part of $\bar{A}_n^R$ which has been neglected in obtaining (A6) as being small compared with the dominant terms in $\lambda_{Eo,}$ does contribute to the integral at $\beta=K_{Eo}$.

The same result can be established directly from Eq. (39), which is an alternate form for Eq. (35). It may be seen that near $\beta=K_{Eo,}$ A/D, which appears in (39), behaves as

$$\frac{A}{D} \longrightarrow \frac{1}{\lambda_{Eo}^2}$$

Thus, the integrand of (39) is independent of $\lambda_{Eo,}$ and therefore integrable at $\beta=K_{Eo}$.

We have so far implicitly assumed a non-zero collision frequency, so that the only singularities of concern are those caused by $\lambda_{Eo.}$ If however, the collision frequency is zero, then while no singularities arise because of λ_E or λ_P becoming zero, as long as $s \neq c$, singularities are instead caused by cancellation of additive terms in D, which while complex for non-zero collision frequencies, become pure real or pure imaginary for zero collision frequency, and thus can have real values of β as roots to $D(\beta) = 0$. Seshadri (1965b) has discussed this question in some detail, so we will not pursue it here.
The free space situation is recovered, so far as the type of singularity is concerned, only if the collision frequency, sheath thickness and electron temperature all become zero.

Appendix B: Error Analysis

Our problem is to obtain a final answer from our integration that is accurate to the desired number of places. If the true answer is F, then we have from (62)

$$F=\sum_{i=1}^{N} f_i \pm E=\tilde{F}\pm E \qquad \text{(B1)}$$

where

$$f_i=\sum_{j=o}^{2^{m+k}}{}' d_{jm} f(a_i+jh)\pm E_i \qquad \text{(B2)}$$

and E is the accumulated convergence error arising from the fact that the contribution of each interval, f_i, is not exactly known due to the convergence error E_i associated with each interval. We assume that the individual $f_{ij}=f(a_i+jh)$ are known as accurately as desired, so that the final accuracy is determined by E_i alone. The problem now is to find a means for specifying the individual allowable E_i in order to keep E within the desired limits.

There are three rather obvious methods that might be used to determine the allowable E_i for each interval. (1) One method would be to keep the convergence error E_i less than a certain fraction of the sum for $\tilde{F}$ to the present interval. (2) A second method would be to determine E_i from the ratio of the largest previous f_i obtained to the present f_i in order to keep the first uncertain figure for each f_i contribution in the same location relative to the decimal point. (3) A third method could be to simply hold

E_i constant throughout. This latter method would be simplest to employ, but less efficient in terms of abscissa points required in comparison with the second. These three methods are examined in turn below.

(1) If we start out with an allowable normalized convergence error per interval of E_C, we then have

$$|E_1| \leqslant E_C |f_1|$$
$$|E_2| \leqslant E_C |f_1+f_2|$$
$$|E_3| \leqslant E_C |f_1+f_2+f_3|$$
$$\vdots$$
$$|E_N| \leqslant E_C |F|$$

then

$$|E| \leqslant E_C|f_1| + E_C|f_1+f_2| + \ldots + E_C|F| \qquad \text{(B3)}$$
$$\leqslant E_C\left[N|f_1| + (N-1)|f_2| + \ldots |f_n|\right]$$

If the f_i are of nearly equal magnitudes (as was actually the case with the variable interval width integration technique) then

$$|E| \leqslant E_C |f_1| \sum_{i=0}^{N-1} (N-i) \qquad \text{(B4)}$$

$$= E_C |f_1| N(N+1)/2$$
$$\approx E_C |f_1| N^2/2$$

Now if all the f_i were of the same sign, then

$$\tilde{F} \approx N f_1$$

so that

$$\left|\frac{E}{F}\right| \approx \left|\frac{E}{\tilde{F}}\right| \approx E_C N/2 \qquad \text{(B4a)}$$

If on the other hand, the f_i alternated in sign, so that

$$|\tilde{F}| \approx |f_1|$$

then

$$\left|\frac{E}{F}\right| \approx \left|\frac{E}{\tilde{F}}\right| \approx E_C N^2/2 \qquad \text{(B4b)}$$

We see that in either case, the normalized error $E_n = |E/F|$ is large. It was not unusual to have N=60, and with $E_C = 2\times10^{-4}$ as was used, then

$$6\times10^{-3} \leqslant E_n \leqslant 0.36$$

(2) We have now

$$|E_1| \leqslant |f_1|\, E_C\, |f_m/f_1|$$
$$|E_2| \leqslant |f_2|\, E_C\, |f_m/f_2|$$
$$\cdot$$
$$\cdot$$
$$\cdot$$
$$|E_N| \leqslant |f_N|\, E_C\, |f_m/f_N|$$

so $$|E| \leqslant E_C N\, |f_m| \qquad \text{(B5)}$$

where f_m is the largest value of f_i. We note that f_m is not a priori known in the actual calculation, since only information on f_i already obtained is available, so that f_m may increase during the course of the summing process. This means that the actual errors may be less than that indicated by (B5),

unless f_m of course happens to be f_1.

Now, if all the f_i were nearly equal and of the same sign,

then

$$\tilde{F} \approx N\ f_1 \approx N\ f_m$$

so

$$\left|\frac{E}{F}\right| \approx \left|\frac{E}{\tilde{F}}\right| \approx E_C \tag{B6a}$$

On the other hand, for alternating f_i, then

$$|\tilde{F}| \approx |f_1| \approx |f_m| \tag{B6b}$$

so

$$\left|\frac{E}{F}\right| \approx \left|\frac{E}{\tilde{F}}\right| \approx N\ E_C$$

Again, for N=60, and $E_C = 2 \times 10^{-4}$, then

$$2 \times 10^{-4} \leqslant E_n \leqslant 0.12$$

(3) In this case

$$|E_1| \leqslant E_C\, |f_1|$$
$$|E_2| \leqslant E_C\, |f_2|$$
$$\cdot$$
$$\cdot$$
$$\cdot\cdot$$
$$|E_N| \leqslant E_C\, |f_N|$$

so

$$|E| \leqslant E_C \left[|f_1| + \ldots + |f_N|\right] \tag{B7}$$

We see that the error here is approximately the same as (B5) for nearly equal f_i. If however, the f_i vary considerably in magnitude, then this

method produces better accuracy. Method 2 was used instead of 3 however, since over most of the range of integration where the major contribution to F arose, the f_i were nearly the same in magnitude, and the two methods are equivalent. In the final stages of the integration, the f_i were rapidly decreasing however, in relation to $\widetilde{F}$, and there is no advantage to finding each f_i to say, 4 significant figures, when the only significant figures in the current $\widetilde{F}$ which will be changed by this f_i, are the last one or two places. Method 2 essentially consists of adding a column of figures given by f_i, with a common decimal point, and having the last significant figure of each f_i fall in the same column.

Since the conductance is obtained from a much smaller integration range than the susceptance, and in addition does not change in sign over that interval, as does the susceptance, it is generally obtained with a higher accuracy. There is also a truncation error associated with the susceptance, which has been previously discussed, (and which has not been considered here in finding E, assumed due alone to the convergence errors of each interval) due to terminating the integration at a finite value of β, further increasing the susceptance error in comparison with the conductance.

We should also mention that the convergence test used here, discussed in section III on the numerical analysis, is a conservative one. It was consistently found that the f_i were accurate to one more significant figure than was indicated by the convergence test. This means that while the actual value used for E_C in the calculations was 2×10^{-4}, the effective E_C was about an order of magnitude less, as was also the resulting accumulated, normalized convergence error E_n. We can thus state that we should

have E_n value arising from our calculations no larger than 10^{-2} in the most unfavorable situation.

Finally, it is worth while to point out that the error testing technique and variable width integration interval technique which were used for these calculations was useful in finding programming errors reflected in the f_i. Any error in the f_i as a function of the integration variable resulted in very small integration intervals in the immediate vicinity of the error. Similarly, specifying E_C to be less than the accuracy with which the f_i were obtained resulted also in very small integration intervals, which oscillated in size. The integration technique developed for these calculations should be very useful and accurate for handling any number of integration problems which involve integrand functions which are time consuming to evaluate.

REFERENCES

Ament, W. S., M. Katzin, J. R. McLaughlin and W. W. Zachary, (1964) Theoretical investigations related to ionospheric probing, Electromagnetic Res. Corp., Rept. No. 1.

Balmain, K. G. (1965), Impedance of a short dipole in a compressible plasma, Radio Sci., J. of Res., NBS/USNC-URSI, 69D, 559.

Bauer, F. L., H. Rutishauser and E. Stiefel (1963), New aspects in numerical quadrature, Experimental arithmetic, high speed computing and mathematics, Vol. 15, Proceedings of Symposia in Applied Mathematics, Amer. Mathematical Soc., Providence R. I.

Bramley, E. N. (October 1965), Measurements of aerial admittance in the ionosphere, Planet. Space Sci. 13, (10) 979 to 995.

Calvert, W. and G. B. Goe (1963), Plasma resonances in the upper ionosphere, J. Geophy. Res., 68, No. 22, 6113-6120.

Chen, Y. and J. B. Keller (1962), Current on and input impedance of a cylindrical antenna, J. of Res. NBS, Section D, 66D, No. 1, 15-21.

Cohen, M. H. (1962), Radiation in a Plasma. III. Metal Boundaries, Phys. Rev., 126, 398-404.

Deering, W. D. and J. A. Fejer (1965), Excitation of Plasma Resonances by a small pulsed dipole, Phys. of Fluids, Vol. 8, No. 11, 2066-2079.

Dougherty, J. P. and J. J. Monaghan (1966), Theory of resonances observed in ionograms taken by sounders above the ionosphere, Proc. Royal Soc. Series A, 289, 214-234.

Duncan, R. H. (1962), Theory of the infinite cylindrical antenna including the feedpoint singularity in antenna current, J. of Res. NBS, 66D, No. 2. 181-188.

Einarsson, Olov (1966), A comparison between tube shaped and solid cylinder antennas, IEEE Trans AP-14, No. 1, 31-37.

Fante, R. L. (1966), On the admittance of the infinite cylindrical antenna, Radio Science, 1, No. 9, 1041-1044.

Fejer, J. A. (1964), Interaction of an Antenna with a hot plasma and the theory of resonance probes, Radio Science J. of Res., NBS/USNC-URSI, 68D, No. 11, 1171-1176.

Fejer, J. A. and W. Calvert (1964), Resonance effects of electrostatic oscillations in the ionosphere, J. Geophy. Res., 69, No. 23, 5049-5062.

Field, G. B. (1956), Radiation by Plasma Oscillations, Astrophysical J., V. 124, 555-570.

Hallen, E. (1930), Uber die elektrischen Swingungen in drahtformigen Leitern, Upsala Universitets Arsskrift, No. 1.

Hallen, J. (1938), Theoretical investigations into the transmitting and receiving qualities of antennae, Nova Acta, Uppsala, 11, No. 4.

Hallen, J. (1939), Further investigations into the receiving qualities of antennae: The absorbing of transient, unperiodic radiation, Uppsala Universitets. Arsskrift, No. 4.

Harp, R. S. and F. W. Crawford (1964), Characteristics of the plasma resonance probe, Microwave laboratory report, Stanford University, ARL-64-139.

Heikkila, W. J. (1965a), Report on a multiple ionospheric probe rocket experiment, Second Conference on Direct Aeronomic Measurements in the Lower Ionosphere, Aeronomy Report 10, University of Illinois, Urbana, Ill.

Heikkila, W. J. (1965b), Impedance and conductivity probes, Second Conf. on Direct Aeronomic Measurements in the Lower Ionosphere, Aeronomy Report 10, University of Illinois, Urbana, Ill.

Heikkila, W. J., J. A. Fejer, J. Hugill, and W. Calvert, (1966) Comparison of ionospheric probe techniques, Southwest Center for Advanced Studies, Auroral Ionospheric Rept., DASS-66-5.

Hessel, A. and J. Shmoys (1962), Excitation of plasma waves by a dipole in a homogeneous isotropic plasma, Proc. Sym. on Electromagnetic and Fluid Dynamics of Gaseous Plasma, 173-183, Polytechnic Press of Poly. Inst. of Brooklyn, New York.

Jackson, J. E. (1952), Rocket-borne instrumentation for ionosphere propagation experiments, NRL Rept. 3909.

Jackson, J. E. and J. A. Kane (1959), Breakdown and detuning of transmitting antennas in the ionosphere, NRL Rept. 5345.

Jackson, J. E. and J. A. Kane (1960), Performance of an RF impedance probe in the ionosphere, J. Geophys. Res. 65, 2209.

Kane, J. A., J. E. Jackson and H. A. Whale (1962), The simultaneous measurement of ionospheric electron densities by CW propagation and RF probe techniques, NASA Tech. Note D-1098.

King, R., C. W. Harrison, Jr., and D. H. Denton, Jr., The electrically short antenna on a probe for measuring free electron densities and collision frequencies in an ionized region. J. of Res., NBS, Sec. D., 65D, No. 4, 371-384.

Kuehl, H. H. (1966), Resistance of a short antenna in a warm plasma, Radio Sci. 1, No. 8, 971-976.

Kuehl, H. H. (1967), Calculations of the resistance of a short antenna in a compressible plasma, Radio Sci. 2, No. 1, 73-76.

Larson, R. W. (1966), A study of the inhomogeneously sheathed spherical dipole antenna in a compressible plasma, PhD thesis, University of Michigan.

Lockwood, G. E. K. (1963), Plasma and cyclotron spike phenomena observed in topside ionograms, Can. J. Phys., 41, p 190-194.

Knecht, R. W., T. E. Van Zandt and S. Russel (1961), First pulsed radio soundings of the topside of the ionosphere, J. Geophy. Res., 66, No. 9, 3078-3081.

Knecht, R. W. and S. Russel (1962), Pulsed radio soundings of the topside of the ionosphere in the presence of spread F, J. Geophys. Res., 67, No. 3, 1178-1182.

MacKenzie, E. C. and J. Sayers (1966), A radio frequency electron density probe for rocket investigation of the ionosphere, Planet. Space Sci., 14, 731-740.

Miller, E. K. and A. Olte (1966a), Excitation of surface currents on a plasma-immersed cylinder by electromagnetic and electrokinetic waves. I. The vacuum sheath, Radio Science, 1, No. 8, 977-993.

Miller, E. K. and A. Olte (1966b), Excitation of surface currents on a plasma-immersed cylinder by electromagnetic and electrokinetic waves. II. The inhomogeneous sheath, Radio Science 1, No. 12, 1425-1433.

Miller, E. K. (1966), Excitation of surface currents on a plasma-immersed cylinder by electromagnetic and electrokinetic waves, U of Mich, Scientific Rept. 05627-4-S.

Miller, E. K. (1967), The admittance dependence of the infinite cylindrical antenna upon exciting gap thickness, submitted to Radio Science.

Ralston, A. (1965), A first course in numerical analysis, McGraw Hill.

Schelkenoff, S. A. (1952), Advanced antenna theory, Chapter 2, John Wiley and Sons, Inc., New York.

Self, S. A. (1963), Exact solution of the collisionless plasma sheath equation, Phys. of Fluids, 6, 1762-1768.

Seshadri, S. R. (1965a), Radiation in a warm plasma from an electric dipole with a cylindrical column of insulation, IEEE, Trans. AP 13, No. 4, 613-629.

Seshadri, S. R. (1965b) Infinite cylindrical antenna immersed in a warm plasma, IEEE, Trans. AP-13, No. 5, 789-799.

Stone, R. G., R. R. Weber and J. K. Alexander (1966a), Measurement of antenna impedance in the ionosphere. I. Observing frequency below the electron gyro frequency, Planet. Space Sci. 14, 631-639.

Stone, R. G., R. R. Weber and J. K. Alexander, (1966b), Measurement of antenna impedance in the ionosphere, II. Observing frequency greater than the electron gyro frequency. Planet. Space Sci. 14, 1007-1016.

Takayama, K., H. Ikegami and S. Miyazaki (1960), Plasma Resonance in a Radio Frequency Probe, Phys. Review Letters, 5, No. 6, 238-240.

Wait, J. R. (1964a), Theory of a slotted sphere antenna immersed in a compressible plasma, Part I, Radio Science J. of Res., NBS/USNC-URSI, 68D, 1127-1136.

Wait, J. R. (1964b), Theory of a slotted sphere antenna in a compressible plasma, Part II, Radio Science J. of Res., NBS/USNC-URSI, 68D, 1137-1143.

Wait, J. R. (1965), On radiation of electromagnetic and electroacoustic waves in a plasma, Appl. Sci. Res., Section B., 12, 1.

Wait, J. R. (1966a), Radiation from a spherical aperture antenna immersed in a compressible plasma, IEEE Trans. AP 14, No. 3, 360-368.

Wait, J. R. (1966b), Theories of Prolate spheriodal antennas, Radio Sci. 1, No. 4, 475-512.

Whale, H. A. (1963), The excitation of electroacoustic waves by antennas in the ionosphere, J. Geophys. Res., 68, 415.